A STRATIGRAPHIC FRAMEWORK FOR LATE CAMBRIAN-EARLY ORDOVICIAN CARBONATE SLOPE TO BASINAL SEDIMENTS IN TYBO CANYON, HOT CREEK RANGE, NEVADA

A Thesis

by

SANDRA G MAREK

Submitted to the Office of Graduate and Professional Studies of
Texas A&M University
in partial fulfillment of the requirements for the degree of

MASTERS OF SCIENCE

Chair of Committee, Michael Pope
Committee Members, Thomas Olszewski
Niall Slowey
Head of Department, John R. Giardino

August 2015

Major Subject: Geology

ABSTRACT

The Cambro-Ordovician Hales Limestone in the Hot Creek Range, Nevada records a carbonate slope to toe-of-slope environment. Gigapan™ photomosaics, measured sections, and thin sections of the outcrops help to identify locations, geometries, and continuity of gravity flow deposits, the primary depositional features in the Hales Limestone. The facies identified in the Hales Limestone are: (1a) clast- and matrix-supported conglomerate-breccia beds, (1b) packstone-grainstone beds, (2) alternating thin, planar calcisiltstone and carbonate mudstone beds, (3) wavy, rippled, and cross-bedded calcisiltstone beds with carbonate mudstone, (4) thin, planar carbonate mudstone, and (5) slumped and folded beds of interbedded carbonate mudstone and calcisiltstone. Where facies 1a has a calcisiltstone matrix, it is interpreted to be a turbidite deposit; where it has a carbonate mudstone matrix, it is interpreted as a debris flow deposit. Facies lb is interpreted to be grain flow deposits. Facies 2-5 are interpreted to record interbedded distal turbidites (calcisiltstone) and background, pelagic carbonate mudstone.

This study focuses on the gravity flow deposits (turbidite and debris flow deposits) in the Hales Limestone. The 80% of gravity flow deposits that are continuous across the outcrop formed as strike-continuous aprons, and the 20% of gravity flow deposits that are not continuous across the outcrop formed as individual depositional lobes. Approximately 85% of these gravity flow deposits were formed by turbidity flows, and 15% were formed by debris flows. The majority of the gravity flow deposits are located in the lower portion of the Hales Limestone.

ACKNOWLEDGEMENTS

I would like to thank my committee chair, Dr. Pope, for his continued support throughout my graduate work at Texas A&M and my committee members, Dr. Olszewski and Dr. Slowey for their guidance on my thesis.

Many thanks also go out to the Berg-Hughes Center and AAPG for providing funding to do field work and prepare thin sections. To my field assistants, Mario Lira and Bobbie Roth, who helped me with everything from mapping bedding and taking readings to carrying rocks, I can't thank you enough; my thesis could not have been done without you.

TABLE OF CONTENTS

LIST OF FIGURES

LIST OF TABLES

INTRODUCTION

Understanding slope sedimentation is becoming increasingly important in the development and exploitation of carbonate reservoirs (Collins et al., 2006; Janson et al., 2011; Katz et al., 2010). The continued development of megafields in the slopes of Tengiz and Poza Rica demonstrate the value of understanding slope depositional processes to better predict reservoir distribution. New insights into slope depositional processes provide improved models for describing and interpreting ancient slope deposits (Playton et al., 2010; Katz et al.; 2010; Verwer et al., 2009; Cook, 1979).

The Hales Limestone, Whipple Cave Formation, and lower House Limestone were previously described by Cook and Taylor (1975, 1977, and 1989). Biostratigraphic correlation based on conodonts and trilobites indicates that the deeper slope facies of the Hales Limestone are coeval with the shallower shelf facies of the Whipple Cave Formation (Taylor and Cook, 1975). The Whipple Cave Formation and lower House Limestone are located in the Central Egan Range, to the east of the Hales Limestone that outcrops in the Hot Creek Range (Figure 1). Shelf and margin sediments from the Whipple Cave Formation were transported basinward and deposited as slope facies in the Hales Limestone at an inferred water depth up to 500 meters (Taylor and Cook, 1977).

This paper describes the lateral continuity and geometries of gravity flow deposits—turbidity flows and debris flows—of the carbonate rocks in this slope/toe-of-slope depositional environment of the Hales Limestone. Three types of deposits are associated with carbonate slopes: debris deposits, grain-dominated deposits, and mud-dominated deposits (Playton et al., 2010). Debris deposits commonly are matrix-supported, but can be matrix to

clast-supported, with very coarse clasts ranging in size from cobbles to boulders. The clasts in debris deposits are very poorly sorted, massive, and ungraded with laminated or massive sediments between clasts (Playton et al., 2010). The sediments, generally from the platform edge and margin, are deposited via debris flow, rockfall, or hyperconcentrated flow. The architecture of these deposits consists of isolated megabreccias, backfilled slope aprons, isolated blocks, megabreccia channels, intercalated scours, discrete tongues, and/or lobe and block complexes (Playton et al., 2010).

Grain-dominated deposits range from very fine sand to pebble size (Playton et al., 2010). The fabrics in these deposits can be fine to coarse skeletal or peloidal grainstone, grainy packstone, and intraclastic or bioclastic grainstone to rudstone. These sediments can be well to poorly sorted, have low angle to planar laminations, may record partial Bouma sequences, and have imbricated or aligned clasts (Playton et al., 2010). These sediments are transported by hyperconcentrated and concentrated flows. These deposits form basinward-fining slope aprons, channel-fan complexes that bypass the toe-of-slope, bypassed lower slope aprons, fans, channel complexes, and slope apron and fan deposits interfingered with basinal sediments (Playton et al., 2010).

Mud-dominated deposits range from clay- to silt-sized grains (Playton et al., 2010). These deposits can contain chert, partial to full Bouma sequences, parallel laminations, bioturbation, hardgrounds, and differential cementation. These sediments were derived primarily from low energy or platform interior environments and the water column. These sediments are transported through suspension and turbidity flows (Playton et al., 2010).

Detailed Gigapan™ photomosaics of the Hales Limestone outcrops illustrate the lateral continuity of these gravity flows and the other slope to basinal facies that create the

defining features of these slope deposits (Figure 2 and 3). Thin section analysis provides information about diagenetic events, sedimentary structures, and faunal constituents of the carbonate mudstone, calcisiltstone, and gravity flow deposits that occur in the slope to basinal facies (Figure 4). This study in the Hales Limestone contributes to the understanding of a slope to basin environment by analyzing the composition, geometries, and continuity of the deposits. This can serve as a model for the characteristics of deposits in deep-water carbonate settings. These carbonate slope to basin deposits are well-exposed in Tybo Canyon of the Hot Creek Range in the southern-central Nevada (Figure 1).

REGIONAL SETTING AND GEOLOGIC HISTORY

During the Neoproterozoic, the North American continent separated from Australia and Antarctica as a result of fragmentation of the supercontinent Rodinia, resulting in the formation of a passive margin on the western edge of Laurentia (Hoffman, 1991). Fluvial and shallow marine sandstone and mudstone deposited off the west coast of Laurentia formed the initial sediments of the evolving passive margin (Levy and Blick, 1989; Ross, 1991; Fedo and Cooper, 2001). The slope and rise of the continental margin on the western side of Laurentia had numerous deep marine turbidity and slump deposits during the Cambrian and Ordovician (Montanez and Osleger, 1993), and the passive margin lasted until the Devonian.

The shallow water carbonates of the Whipple Cave Formation and lower House Limestone (Figure 1) that outcrop in the Egan Range in eastern Nevada record a shoal and peritidal depositional environment on a carbonate shelf (Cook and Taylor, 1977). The lower 200 m of the Whipple Cave Formation is primarily argillaceous limestone containing trilobites, sponge spicules, lime mud, and peloids, representing a shallow, low energy subtidal environment on an open shelf with abundant tidal flats and very little wave action in well-oxygenated waters. The upper 380 m of the Whipple Cave Formation contains significant algal buildups that interfinger with fenestral and ribbon limestone, indicating moderately high energy environments (Cook and Taylor, 1977).

The uppermost unit of the shallow water sediments, the lower 50 m of the House Limestone, is composed of dolomitic lime mudstone and fenestral mudstone alternating with channels filled with breccia and conglomerate that formed in a tidal flat environment (Cook and Taylor, 1977). The shallow water sediments in the Egan Range were deposited in

shallow subtidal to supratidal environments. The carbonate platform was ocean-facing and deepening westward based on the relative location of the deep and shallow water carbonate facies in the Egan Range (Cook and Taylor, 1977). The coeval deep water carbonates of the Hales Limestone were deposited in the Hot Creek Range in central Nevada (Cook and Taylor, 1977).

METHODS

Five detailed stratigraphic sections were measured in Tybo Canyon in August 2012 and May 2013: four in the cliff exposure on the north side of the canyon and the fifth on a small outcrop on the west side of the canyon (Figure 5). Measured section descriptions include the size, orientation, composition of grains and clasts of the re-deposited sediments, sedimentary structures, fossils, and bioturbation in the Hales Limestone deposits.

Rock samples were collected throughout the measured sections, and they were described using the Dunham (1962) classification with modification from Embry and Klovan (1972). Thin sections from the rock samples were used to determine petrographic features of the rocks. The thin sections helped to identify small-scale sedimentary structures and depositional and diagenetic features (Figure 4).

Lateral continuity of the Hales Limestone beds was mapped using Gigapan™ photomosaics and walking out the beds to determine the continuity and geometries of the conglomerate beds that record turbidite and debris flow deposits. The Gigapan™ software stitches together a series of photographs to create detailed photomosaics of the Hales Limestone outcrops in Tybo Canyon. These photomosaics include images of the large cliff exposure of the Hales Limestone, two separate large cliff faces of the main Hales Limestone exposure (Figure 2), and the small hill in the west side of Tybo Canyon (Figure 3).

DISCUSSION

Sediment, Grain, and Fossil Types

The sediments of the Hales Limestone are primarily carbonate, but there are also a variety of other types of grains as well as later diagenetic alterations to the primary sediments. The majority of the Hales Limestone contains relatively few fossils, occurring in the matrix and clasts of some of the gravity flow deposits. Macrofossils that do occur include calcite and silica sponge spicules, trilobites, brachiopods, gastropods, and crinoids. There also are numerous calcispheres (Scholle and Ulmer-Scholle, 2003), whose abundance varies in different layers. Insoluble residue and styolites that occur throughout the Hales Limestone indicate that there is a significant amount of post-depositional compaction and dissolution of the carbonate sediments (Scholle and Ulmer-Scholle, 2003).

Detrital siliciclastic silt grains, which are likely terrestrially sourced (Dilliard, 2010; Cook and Taylor, 1977), are typically scattered throughout the different rock and bed types. Chert in the Hales Limestone occurs throughout the outcrop as either continuous to semi-continuous layers (typically 1-5 cm thick) or nodules (as small as 3 cm). The chert layers in the Hales Limestone are generally more highly fractured than the surrounding sediments, and these fractures often are filled with calcite cement. Sparry calcite usually occurs as the result of recrystallization of fine-grained sediments, most likely originally carbonate mudstone and calcisiltstone.

The Hales Limestone also contains iron-rich ankerite (yellow/reddish in thin section) and pyrite (dark red in thin section) grains. Euhedral ankerite crystals replace some carbonate mud and calcite that fills fractures and veins, indicating that it formed at a late stage of

diagenesis. The pyrite was formed in an iron-reducing environment, precipitating and replacing carbonate grains during surface exposure.

The majority of the ankerite and pyrite in the Hales Limestone were a result of secondary replacement of carbonate sediments. This is indicated by the random crystal replacement of ankerite and pyrite grains in the carbonate sediments. In addition, fractures in the Hales Limestone can be either primary or secondary. Some fractures may be the result of the sediment movement during the time of deposition, but the abundance of fractures throughout the bedding of the Hales Limestone indicates that majority of the fractures are secondary features.

Facies

Five facies (Table 1) comprise the Hales Limestone: 1a) clast- and matrix-supported conglomerate-breccia,1b) packstone-grainstone, 2) alternating thin, planar calcisiltstone and carbonate mudstone, 3) wavy and cross-bedded mudstone and calcisiltstone, 4) thin planar mudstone, and 5) deformed of carbonate mudstone and calcisiltstone.

1a) Clast- and matrix-supported conglomerate-breccia facies

Description- The clast- and matrix-supported conglomerate-breccia facies generally has beds 20 cm to 3 m thick. Calcisiltstone composes the majority of the matrix in the conglomerate clast beds with the remainder composed of carbonate mudstone and peloids. The conglomerate beds in the Hales Limestone are primarily composed of silt- to pebble-sized grains, indicative of a grain-dominated deposit. Six stacked clast beds compose 20% of the conglomerate clast beds of facies 1a in the main outcrop of the Hales Limestone. Clasts in the conglomerate beds from the Hales Limestone have a length to width ratio ranging from

1:1 to 20:1, but the majority of these clasts have a length to width ratio between 1:1 and 5:1. These clasts are generally elongated sections of sediment with longer length and height and significantly shorter width, forming flat-pebble conglomerate-breccia clasts. The conglomerate beds in the Hales Limestone show variations in continuity in addition to lateral and vertical thickness variations. The scouring base of these deposits often creates undulating bed contacts at the bottom of the beds (Figures 6 and 7).

Interpretation- 85% of these clast beds are deposits of the first stage (A) of the turbidite sequence, and the other 15% are composed of debris flow deposits. The mud matrix and coarse clasts of the debris flows are indicative of debris deposits. The majority of the continuous, clast-supported conglomerate-breccia beds in the Hales Limestone are interpreted as grain-dominated aprons forming laterally continuous sheets. The calcisiltstone matrix, pebble- to boulder-sized clasts, normal and inverse grading, and stacked conglomerate-breccia beds (Figures 7 and 8) in the Hales Limestone also indicate grain-dominated flows. The grain flow deposits that form laterally continuous aprons across the exposed outcrop of the Hales Limestone are interpreted as turbidite deposits. The grain flow deposits that form laterally discontinuous lobes on the Hales Limestone are primarily interpreted as debris flow deposits. In the Hales Limestone, debris flow deposits, facies 1a, are primarily clast-supported, but the ratio of matrix to clasts in these deposits is higher than that of turbidites.

1b) Packstone-grainstone facies

Description-The packstone to grainstone facies are composed of brachiopod, trilobite, gastropod, crinoid, and peloid grains with micrite and calcite matrices. These highly fractured beds are primarily located on the eastern portion of the Hales Limestone in Tybo

Canyon, and are composed of fossil and peloidal packstone to grainstone deposits. The Hales Limestone outcrops on the north and west side of Tybo Canyon contain fossils in 25% of the clast beds and thin beds. The abundance of these shallow water deposits containing fossils and peloids and the conglomerate-breccia beds decreases moving upslope.

Interpretation- These beds are high-energy grain flow deposits that originated in a shallow water margin to shelf environment.

2) Alternating thin, planar calcisiltstone and carbonate mudstone facies

Description- Sediment layers in the alternating dark and light thin, planar carbonate mudstone and calcisiltstone facies typically ranges in thickness from thin bedded (7 cm) to laminated (2mm), though bedding can range from 1 m to 100 m thick. These beds are often deposited in association with the sediments from facies 1a.

Interpretation- These facies may be lower energy than, facies 1a, but the large amount of calcisiltstone and low amount of carbonate mudstone indicates an intermediate- to high-energy environment, likely episodic, during deposition. The alternating layers of calcisiltstone and carbonate mudstone, facies 2, in the Hales Limestone represent the second (B) stage of the carbonate turbidite sequence (Figure 9). The layering of these sediments represents deposition as a result of decreased energy from the gravity flow after the larger clasts were deposited out of the suspended sediments

3) Wavy and cross-bedded mudstone and calcisiltstone facies

Description- Beds of the wavy and cross-bedded mudstone and calcisiltstone facies range from 50 cm to 1 m thick. The abundance of calcisiltstone allows the cross-bedding, climbing ripples, and wavy bedding to form and be preserved. These calcisiltstone beds often occur directly above the clast beds, facies 1a.

Interpretation- Based on the low-angle cross-laminations and large amount of calcisiltstone, these beds were deposited episodically in an intermediate- to high-energy environment. This environment either does not have enough energy to move coarse grains such as the environment in the first stage (A) of the carbonate turbidite sequence, or the coarser sediments from the same gravity flow were already deposited. The wavy beds in the Hales Limestone, facies 3, represent the third stage (C) stage of the carbonate turbidite sequence (Figure 9). These beds are often associated with the clast-supported beds of facies 1, but lack the lateral continuity of the conglomerate-breccia clast beds (facies 1a).

4) Thin planar mudstone facies

Description- Beds of the thin planar mudstone facies range in thickness from 2 cm to 10 cm. These layers of thin-bedded carbonate mudstones can form continuous sections up to 70 m thick. They lack the calcisiltstone that is prevalent in facies 2. Some of the carbonate mudstone contains interbedded chert. In this facies, some of the uppermost beds of these thin-bedded carbonate mudstone layers also have horizontal burrows and fossils, indicating an environment shallow enough to allow organisms to live. Although the deposits for the second (B) and fourth (D) stages of the carbonate turbidite sequence can be similar in the Hales Limestone, the deposits of the fourth stage (D) have an increased mud content.

Interpretation- The significant variations in bed thickness of the planar carbonate mudstone suggest that they were deposited as distal turbidites. The thin-bedded carbonate mudstone, facies 4, represents the upper stage (D) of the carbonate turbidite sequence or the background sedimentation on the slope environment (Figure 9). This carbonate mudstone was deposited in a calm, low-energy environment as thin beds as pelagic rain out in front of the carbonate platform or as mud settling out of the water after a turbidity flow. It is possible

that the fossils were re-deposited from upslope, like those in the clast beds, but the occurrence of burrows indicates living organisms at or soon after the time of deposition.

5) Deformed carbonate mudstone and calcisiltstone facies

Description- Beds of the deformed carbonate mudstone and calcisiltstone facies range from 0.5 m to 100 m thick and feature soft-sediment folding and slumping.

Interpretation- The folding and slumping features in these facies suggests that these deposits formed as a result of sediment instability. The soft sediment deformation may also be a result of sediment compaction, and folding may be a result of deformation during uplift.

Facies Associations and Successions

The predominant sediment type deposited in the Hales Limestone is thin-bedded carbonate mudstone (Figure 10), interpreted to have been deposited in water depths up to approximately 500 meters based on Reinhardt's (1977) study of Cambrian slope to basinal sediments in the central Appalachians, modern continental slopes, and faunal data in relation to the location of the thermocline (Cook and Taylor, 1975; Cook and Taylor, 1977; Cook and Enos, 1977). These sediments, primarily composed of carbonate, were deposited as a result of pelagic settling from the water column.

Facies 1a and 1b are more abundant in the lower portion of the Hales Limestone than in the upper portion. In the lower half of this outcrop, facies 1 comprises 35% of the Hales Limestone and 25% of the total exposure of the Hales Limestone (Figure 2). Facies 2 and 4 are difficult to differentiate in outcrop and, combined, comprise the majority of the Hales Limestone: 70% of the lower half of the Hales Limestone. Facies 3 and is not abundant on the outcrop and comprises approximately 5% of the Hales Limestone.

The abundant gravity flow deposits in the Hales Limestone indicate a slope carbonate environment with a geometry between that of a ramp and a rimmed platform (e.g. Read 1985). There are no apparent scarps or scallops on the Hales Limestone outcrop to indicate a very steeply rimmed carbonate platform, but the presence of gravity flow deposits indicates a depositional environment steep enough to create sediment instability. The lithology changes from the Dunderberg Shale to the Hales Limestone indicates a transition from a basinal to a slope setting.

Depositional Model

Gravity flow deposits in the Hales Limestone are composed of turbidites and debris flow deposits. Turbidites in carbonate sediments vary slightly from those in siliciclastic sediments (Krause and Oldershaw, 1978). Turbidity currents occur when sediment flows downslope and become suspended in water (Middleton, 1993). Turbidites are deposited from suspension. At the front end of a turbidity flow, the sediments from the slope are eroded, creating scour features at the base of the bed. After erosion, beds of the coarser sediments—conglomerate and breccia clasts—are deposited.

The submarine conglomerate-breccia bed sequences from carbonate turbidites involve disorganized clasts, disorganized stratified clasts, and normally or inversely to normally graded stratified sediments. The matrix for these coarse-grained deposits is primarily silt and calcisilt. The silt-sized grains allow water to mix between the sediment and allow the turbulence and tumbling of clasts during the flow (Middleton, 1993). Clasts of turbidity currents originating on a slope are composed of fragments of the mudstone and siltstone, and

clasts that originate in shallower waters are composed of wackestone, packstone, and bioturbated sediments (Bouma, 1962; Krause and Oldershaw, 1978). Intervals A (large massive to graded sediments and clasts), B (plane parallel layers of sand to silt-sized grains), and C (ripples, wavy bedding, and convoluted bedding) of the Bouma sequence are the equivalent predominant sediment deposits of the turbidites (Figure 9) in carbonate environments (Bouma, 1962; Krause and Oldershaw, 1978; Middleton, 1993).

The graded bedding associated with the turbidity flows in the Hales Limestone includes fining-upward and coarsening-upward sequences of clasts and coarsening upward sediments (Figure 8). Complete turbidite sequences are rare in the Hales Limestone, but partial sequences occur commonly. Parts A, B, and D are the most commonly preserved sections of the turbidite sequence in the Hales Limestone, though part C also is relatively abundant (Figure 9). Low-angle cross bedding and climbing ripples occur above some of the thicker and better-exposed clast beds, but often only beds of conglomerate clasts record the gravity flow deposits. In the Hales Limestone, up to 24% of the conglomerate clast beds, part A of the turbidite sequence, are overlain by cross-bedding, climbing ripples, or wavy bedding recording part C of the carbonate turbidite sequence.

The conglomerate clasts of these gravity flow deposits are composed almost exclusively of carbonate mudstone and calcisiltstone. These are primarily grain-dominated deposits composed of calcisiltstone, granules, pebbles, and cobbles. Calcisiltstone is the majority of the matrix with carbonate mudstone comprising a smaller fraction. The similar and consistent composition of the clasts and matrix indicates that these sediments were previously deposited on the slope and subsequently re-worked.

The gravity flow deposits in the Hales Limestone are interpreted to be predominantly calcareous turbidites. The turbidite are primarily interpreted based on the conglomerate facies 1a deposits that have a calcisiltstone matrix. Graded bedding, cross bedding of laminated mudstone and siltstone, and climbing ripples are additional factors when interpreting gravity flow deposits as turbidites (Figure 9). Debris flows are less common than turbidites in the Hales Limestone, and they are identified by large boulders of thin bedded carbonate mudstone and calcisiltstone and a primarily mudstone matrix (Figure 6).

The majority of the gravity flow deposits in the Hales Limestone are interpreted to be continuous across the Tybo Canyon outcrops; conglomerate clast beds that are a few centimeters to tens of centimeters thick can be correlated across a majority of the outcrop (over 800 m). 40% of the clast beds on the Hales Limestone outcrop in Tybo Canyon terminate within the expanse of the outcrop. This percentage of pinch outs of these clast beds is interpreted based on visible terminations and talus and covered intervals on the outcrop obscuring the continuity of these beds.

Some small- to intermediate-scale, discontinuous conglomerate-breccia can be interpreted as both apron and lobe deposits (Figure 10). These conglomerate-breccia clast beds also form stacked turbidite deposits, which are typically associated with apron deposits (Figure 7). The gravity flow deposits that form debris flows likely originate at a point source, and the difference in sediment suspension between turbidites and debris flows causes the gravity flows to form different geometries upon deposition of the sediments (Playton et al., 2010)

The deformed beds of the Hales Limestone, which consists of planar beds, indicate small-scale movement of the sediments. Some deposits show only slight deformation where

layers of sediment were broken apart, with only a slight separation between the clasts (Table 1). This slight deformation of the sediments bounded above and below with planar sediments allows for the interpretation of the original position of the sediments. Other beds show significant deformation of the sediments. The folding and slumping in the beds indicate deformation of the sediments across a spectrum of conditions. These sediments likely underwent a similar process to that which forms the turbidity flow and debris flow deposits. The sense of motion of the deformed beds is similar to that of the turbidity and debris flow deposits, but the effects of these events in the deformed beds are not as intense or widespread as those in the clast bed deposits (Table 1). Larger bed-scale deformation is a result of gravity instabilities, while the smaller soft-sediment deformation is a result of sediment loading and compaction.

There is an abrupt sea level drop following a global sea level rise during the Sauk Sequence in the Cambrian. There is another global sea level rise during the Tippecanoe Sequence that starts in the Ordovician. Localized regressions occur in the Middle Ordovician with a continued rise in sea level into the Silurian (Vail et al., 1977). The upslope decrease of conglomerate-breccia clast beds and shallow water sediments in the Hales Limestone of the Hot Creek Range likely indicates a sea level rise. The abundance of gravity flow deposits and shallow water clasts at the base of the Hales Limestone likely records a decrease in accommodation space leading to sediment shedding off the carbonate platform onto the slope and into the basin. The decrease in gravity flow deposits up section and the fining of sediments deposited on the slope and toe-of-slope environment suggests rising sea level and drowning of the platform margin. The reoccurrence of some gravity flow deposits and

shallow water sediments at the top of the Hales Limestone may record the beginning of a subsequent decrease in water depth.

CONCLUSIONS

This study shows the variation and complexity of deposits in this carbonate slope to basinal setting. Detailed mapping of the outcrops and photomosaics helped to create an outcrop-scale depiction of the location and extent of the gravity flow deposits, which provides a better understanding of how these flows occur and predicting their extent. The gravity flow deposits are composed of both turbidites and debris flows. Gravity flow deposits in the Hales Limestone, identified by conglomeratic-breccia beds, are both continuous and discontinuous where they are exposed in Tybo Canyon. The laterally continuous conglomerate deposits are indicative of aprons, and the laterally discontinuous conglomerate deposits are indicative of lobe deposits.

The majority of these gravity flow deposits have a calcisiltstone matrix, and numerous conglomerate-breccia beds are overlain with high-energy beds indicated by calcisiltstone deposits of wavy bedding, ripple marks, and cross bedding. This sequence of sediment layers is indicative of turbidites, indicating that the majority of the conglomerate-breccia clast deposits are a result of turbidity flows. The grain-dominated deposits containing calcisiltstone and clast-supported matrix comprise 85% of the conglomerate-breccia clast deposits, indicative of turbidites. The other 15% of the conglomerate-breccia clast beds with mud matrix and coarse to very coarse clasts are debris flow deposits. The same process that causes the large-scale gravity flow deposits also produced smaller-scale slumped and deformed beds.

The clasts from the conglomerate beds are composed of the same types of carbonate mudstone and calcisiltstone sediments that are deposited as normal sedimentation for the

carbonate slope, indicating that they are composed of sediments previously deposited in a slope setting. Trilobites, brachiopods, gastropods, and crinoids are in some of the carbonate gravity flow sediments, indicating that these fossils are likely the result of sediment flows that sourced shallower water sediments. The sediments of the gravity-flow deposits on the east side of Tybo Canyon composed of skeletal and peloidal grainstones and packstones also originated from shallower water sediments.

REFERENCES

Bouma, A. H., 1962, Sedimentology of some flysch deposits: A graphic approach to facies interpretation, Elsevier Publishing Co., 168 p.

Collins, J.F., Kenter J.A.M., Harris, P.M., Kuanysheva, G., Fischer, D.J., Steffen, and K.L., 2006, Facies and reservoir-quality variations in the late Visean to Bashkirian outer platform, rim, and flank of the Tengiz buildup, Precaspian Basin, Kazakhstan: in P.M. Harris and L.J. Weber, eds., Giant hydrocarbon reservoirs of the world: From rocks to reservoir characterization and modeling, AAPG Memoir 88/SEPM Special Publication, p. 55-95.

Cook, H.E. and Taylor, M.E., 1975, Early Paleozoic continental margin sedimentation, trilobite biofacies, and the thermocline, western United States: Geology, v. 3 p. 559-562

Cook, H.E. and Taylor, M.E., 1977, Comparison of continental slope and shelf environments in the Upper Cambrian and Lowest Ordovician of Nevada. in H.E. Cook (ed.) and P. Enos (ed.) Deep-Water Carbonate Environments. Society of Economic Paleontologists and Mineralogists Special Publication No. 25, 1977. p. 51-81.

Cook, H. E., 1979, Ancient continental slope sequences and their value in understanding modern slope development: The Society of Economic Paleontologists and Mineralogists (SEPM), Special Publication No. 27, p. 287-305.

Cook, H.E., Taylor, M.E., and Miller, J.F., 1989, Day 2: Late Cambrian and Early Ordovician stratigraphy, biostratigraphy and depositional environments, Hot Creek Range, Nevada: in M.E. Taylor (ed.) Cambrian and Early Ordovician Stratigraphy

and Paleontology of the Basin and Range Province, Western United States, Guidebook for Field Trip T125, 28th International Geological Congress, p. 28-36.

Dilliard, K. A., Pope, M. C., Coniglio, M., Hasiotis, S. T., and Lieberman, B. S., Active synsedimentary tectonism on a mixed carbonate-siliciclastic continental margin: third-order sequence stratigraphy of a ramp to basin transition, lower Sekwi Formation, Selwyn Basin, Northwest Territories, Canada: Sedimentology, v. 57, p. 513-542.

Dunham, R. J., 1962, Classification of carbonate rocks according to depositional texture, American Association of Petroleum Geologists Memoir, p. 108-121.

Embry, A. F. and Klaven, J. E., 1971, A Late Devonian reef tract on northeastern Banks Island, N.W.T.: Bulletin of Canadian Petroleum Geology, v. 19, p. 730-781.

Fedo, C. M. and Cooper, J. D., 2001, Sedimentology and sequence stratigraphy of Neoproterozoic and Cambrian units across a craton-margin hinge zone, southeastern California, and implications for the early evolution of the Cordilleran margin: Sedimentary Geology, p. 501-522.

Hoffman, P.F., 1991, Did the breakout of Laurentia turn Gondwanaland inside-out?: Science, v. 252, p. 1409–1412.

Janson, X., Kerans, C., Loucks, R., Marhx, M. A., Reyes, C., and Murguia, C., 2011, Seismic architecture of a Lower Cretaceous platform-to-slope system, Santa Agueda and Poza Rica fields, Mexico: *AAPG Bulletin*, v. 95, p. 105-146.

Katz, D.A., Playton T., Bellian, J., Harris, P.M., Harrison, C., Maharaja, A., 2010, Slope Heterogeneity in a Steep-Sided Upper Paleozoic Isolated Carbonate Platform Reservoir, Karachaganak Field, Kazakhstan, Abstract, conference paper, SPE

Caspian Carbonates Technology Conference, 8-10 November 2010, Atyrau, Kazakhstan,

Krause, F. F. and Oldershaw, A. E., 1978, Submarine carbonate breccia beds—a depositional model for two-layer, sediment gravity flows from the Sekwi Formation (Lower Cambrian), Mackenzie mountains, Northwest Territories, Canada: Canadian Journal of Earth Sciences, v. 16, p. 189-199.

Levy, M. and Blick, N., Pre-Mesozoic palinspastic reconstruction of the eastern Great Basin (Western United States): Science, v. 245, p. 1451-1462.

Montanez, I. P. and Osleger, D. A., 1993, Parasequence Stacking Patterns, Third-Order Accommodation Events, and Sequence Stratigraphy of Middle to Upper Cambrian Platform Carbonates, Bonanza King Formation, Southern Great Basin: AAPG Memoir, v. 57, Carbonate Sequence Stratigraphy: Recent Developments and Applications, p. 305-326.

Playton T.E., Janson, X., Kerans, C., 2010, Chapter 18: Carbonate Slopes. In N.P. James (ed.) and R.W. Dalrymple (ed.) Facies Models 4, Geologic Association of Canada, 2010. p. 449-476.

Read, F.J., 1985, Carbonate Platform Facies Models: AAPG Bulletin, v. 69, No. 1, p. 1-21.

Reinhardt, J., 1977, Cambrian Off-Shelf Sedimentation, Central Appalachians: SEPM Special Publication, No. 25, p. 83-112.

Ross, G.M., 1991, Tectonic setting of the Windermere Supergroup revisited: Geology, v. 19, p. 1125-1128.

Scholle, P. A. and Ulmer-Scholle, D. S., 2003, A color guide to the petrography of carbonate rocks: grains, textures, porosity, diagenesis: AAPG Memoir, v. 77.

Vail, P.R., Todd, R.G., and Sangree, J.B., 1977, Seismic Stratigraphy and Global Changes of Sea Level: Part 4. Global Cycles of Relative Changes of Sea Level: Section 2. Application of Seismic Reflection Configuration to Stratigraphic Interpretation: AAPG Memoir, v. 26.

Verwer,K., Merino-Tomé, O., Kenter, J.A.M., 2009, Evolution of a High-Relief Carbonate Platform Slope Using 3D Digital Outcrop Models: Lower Jurassic Djebel Bou Dahar, High Atlas, Morocco: Journal of Sedimentary Research, v. 79, p. 416-439.

APPENDIX A

FIGURE CAPTIONS

Figure 1: Location map, stratigraphic section, and photomosaic of Hales Limestone in Hot Creek Range, Nevada.

A) Location map of this study of the Hales Limestone. Tybo Canyon, Hot Creek Range, Nevada is located off of Nevada Hwy 6 between Tonopah, NV and Ely, NV.
B) Stratigraphic column of the Hales Limestone and Dunderberg Shale in Hot Creek Range in relation to coeval shallow water sediments of the Whipple Cave Formation and House Limestone in Central Egan Range, Nevada (adapted from Cook & Taylor, 1975 & 1977).
C) Google Earth™ image showing the exposed outcrop of the Middle-Late Cambrian Hales Limestone in Tybo Canyon, Hot Creek Range, Nevada. The yellow lines indicate the locations of measured sections. The measured sections are labeled as "Hill," "MS 6," "C1," "C2," and "MS 8." The hill with the exposed Hales Limestone is located at the bottom left corner of the image. The main outcrop of the Hales Limestone is located in the upper central portion of this image.

Figure 2:

Gigapan™ photomosaic of the main outcrop of the Hales Limestone located on the north side of Tybo Canyon. The image is taken using a Nikon Digital SLR camera with a 300 mm lens connected to a Gigapan™ device. The blue shapes on the image indicate the location, continuity, and geometries of the gravity flow deposits located on this outcrop. The lack of continuity across the entirety of this outcrop exposure is because of talus slopes that

cover the outcrop, locations where the outcrop is not exposed at the surface, and discontinuous gravity flow deposits. Gravity flow deposits were interpreted across some of the covered sections, blue and white hash marks, on the outcrop where the deposits can be seen across the covered interval. The remaining exposed rocks in this figure, including the large cliff in the upper portion of the outcrop, are composed of carbonate mudstone and calcisiltstone. The locations of measured sections C 1, C 2, and MS 8 are indicated by yellow lines on the outcrop. The white dashed line indicates the approximate boundary between the Dunderberg Shale, below, and the Hales Limestone, above.

Figure 3:

Photomosaic of the small outcrop of the Hales Limestone located on the west side of Tybo Canyon. The blue shapes on the image indicate the location, continuity, and geometries of the gravity flow deposits on this small outcrop. There is a lack of continuity between some outcrop exposures. The discontinuous sections could be a result discontinuous gravity flow lobes or covered sections of the Hales Limestone outcrop. Some gravity flow deposits were interpreted across covered intervals, hashed blue and white lines, where there is continuity of deposit type, shape, and geometry. The yellow line indicates the location of the measured section on this outcrop.

Figure 4: Hand sample and photomicrographs of Hales Limestone.

A) Scanned thin section of silica-rich layers interbedded with carbonate mud. The layers with more abundant silica grains are darker, wider in this image, and they are uneven.
B) Fossils occurring in a skeletal packstone bed of the Hales Limestone. Brachiopod (B), trilobite (T), and gastropod (G).

C) Multiple oblong calcispheres in a carbonate mudstone. There are fragments of organic matter and insoluble residue scattered throughout the carbonate mudstone.

D) A styolite of organics and insoluble residue separates a layer of mudstone with a spicule (upper left) from a layer of calcisiltstone (bottom left).

E) Dark red, cubic pyrite in the Hales Limestone. The pyrite typically occurs in the carbonate mudstone.

F) Monaxial and triaxial sponge spicules in the carbonate mudstone. The spicules in the Hales Limestone are composed of both calcite and silica.

G) Yellowish-orange rhombohedral ankerite grains in carbonate mudstone.

H) Peloid calcisiltstone clast on the right 2/3 of the image and peloids in calcite cement on the left 1/3 of the image. This image is under cross nichols and a gypsum plate.

Figure 5:

Two measured sections of the Hales Limestone outcrop. The locations of the measured sections are located on Figure 1. C1 beds have a strike and dip of approximately 270 N, 20° NE. The hill beds have a strike and dip of approximately 235 N, 32° SE. The presence of shallow water clasts and conglomerate-breccia clast beds decreases upslope.

Figure 6:

A debris flow mega-breccia clast (MBC). This clast is outlined in white and occurs partially in a clast-supported turbidite deposit and partially on the thin-bedded sediments (TBS) that underlie the clast-supported breccia (CSB) bed. This clast, at its maximum, is approximately 2 meters high and 8 meters long. The white box indicates a rock hammer for scale. The MBC is composed of interbedded carbonate mud and calcisiltstone, indicating that the source of this deposit was the slope.

Figure 7: Geometry of beds

A) The sharp termination of a turbidite deposit (right) adjacent to thin-bedded mudstone (left). The thin-bedded sediments (TBS) are curved adjacent to the clast-supported breccia (CSB) deposit. This indicates that the thin-bedded sediments on the left side of the image were either deposited before the turbidite scoured away the sediment and that the thin-bedded sediments were only partially lithified when the turbidite flow occurred or the thin-bedded sediments were curved during sediment compaction.

B) Gravity flow deposits (GFD) are stacked with the lower white line indicating the boundary between thin-bedded sediments (TBS) and the first gravity flow deposit. The upper white line indicates the boundary between 2 separate gravity flow deposits. Both gravity flow deposits scour into the beds upon which they were deposited.

C) Gravity flow deposit scouring the underlying thin-bedded sediments. This gravity flow deposit is a turbidite, as indicated by the scouring and the calcisiltstone matrix of the clast bed. There is a range of clast sizes and orientations within this turbidite deposit.

Figure 8: Outcrop photos of gravity flows, Hales Limestone

A1) Conglomerate and breccia carbonate mudstone and calcisiltstone clasts in a calcisiltstone matrix. This clast bed is deposited above a very thin-bedded layer of carbonate mudstone.

A2) Normally graded carbonate mud conglomerate and breccia clasts in a calcisiltstone matrix. The clasts range in size from 8 cm to < 1cm.

B1) Thin-bedded layers of calcisiltstone and carbonate mudstone transition upward into an irregular layering of carbonate mudstone and calcisiltstone. The thin-bedded

layers are primarily composed of calcisiltstone. The calcisilt grains in the carbonate mudstone of the upper half of the image indicate the amount of energy in which the sediments were deposited.

C1) Climbing ripples composed of calcisiltstone and carbonate mudstone. The contrast between the prevalent calcisiltstone and the carbonate mudstone illustrates the high-energy environment in which these sediments were deposited and allow the sedimentary structures to be more-readily seen.

C2) Cross bedding of calcisiltstone in carbonate mudstone. The layers of calcisiltstone are deposited at a low angle in the carbonate mudstone. These sediments are deposited on top of a bed of conglomerate and breccia clasts.

D1) Thin-bedded carbonate mudstone. These sediments often form large, continuous sections of sediment and are cliff-formers.

Figure 9: Idealized turbidite deposit in the Hales Limestone

The majority of the gravity flow deposits in the Hales Limestone are turbidites. This image, modified from Krause and Oldershaw (1978) represents the idealized types of deposits that result from turbidity flows in deep water carbonate environments such as the Hales Limestone. There are four stages of this flow sequence, from A to D. Examples of these types of deposits, A1 – D1, are represented in Figure 8 with their relative location indicated on the left side of the figure.

A) This is generally represented by conglomerate and breccia clasts ranging in size from granule to boulders. Disorganized and chaotically-organized clasts (A1) are the most

abundant form of deposition at this stage. Normal grading (A2) and inverse grading of clasts also occur in this stage of deposition.

B) This is represented by thin-bedded layers of carbonate mudstone and calcisiltstone (B1).

C) This shows movement of the sediments in a high-energy environment as indicated by soft sediment deformation, climbing ripples (C1), and cross-bedding (C2). The sediments deposited at this stage tend to have a higher abundance of calcisiltstone than carbonate mudstone.

D) The sediments in this stage are similar to those of stage B, but stage D has a higher abundance of carbonate mud. Stage D has thin to very thin bedding (D1). These sediments are often indistinguishable from the background sedimentation of pelagic mudstone.

Figure 10:

The block diagram illustrates shallow to deeper water sediments from the Central Egan Range to the Hot Creek Range during the deposition of the Hales Limestone. There is pelagic to hemi-pelagic rain out on the slope to basinal sediments in the Hot Creek Range that provide the background sediment layers of mudstone that forms the majority of the clasts of the gravity flow deposits. The majority of the gravity flows originate on the slope as a result of instability in the sediments. This same process occurs on a smaller scale with slumped beds in the thin-bedded sediments. These are gravity flow deposits that originate from shallower water indicated by a larger abundance of peloidal calcisiltstone and fossils fragments in some clasts. The slope and shelfal deposits were modified from Cook and

Taylor (1975) to better represent the gravity flow deposits from this study and an updated understanding of shallow water carbonate environments.

APPENDIX B

FIGURES

Figure 1

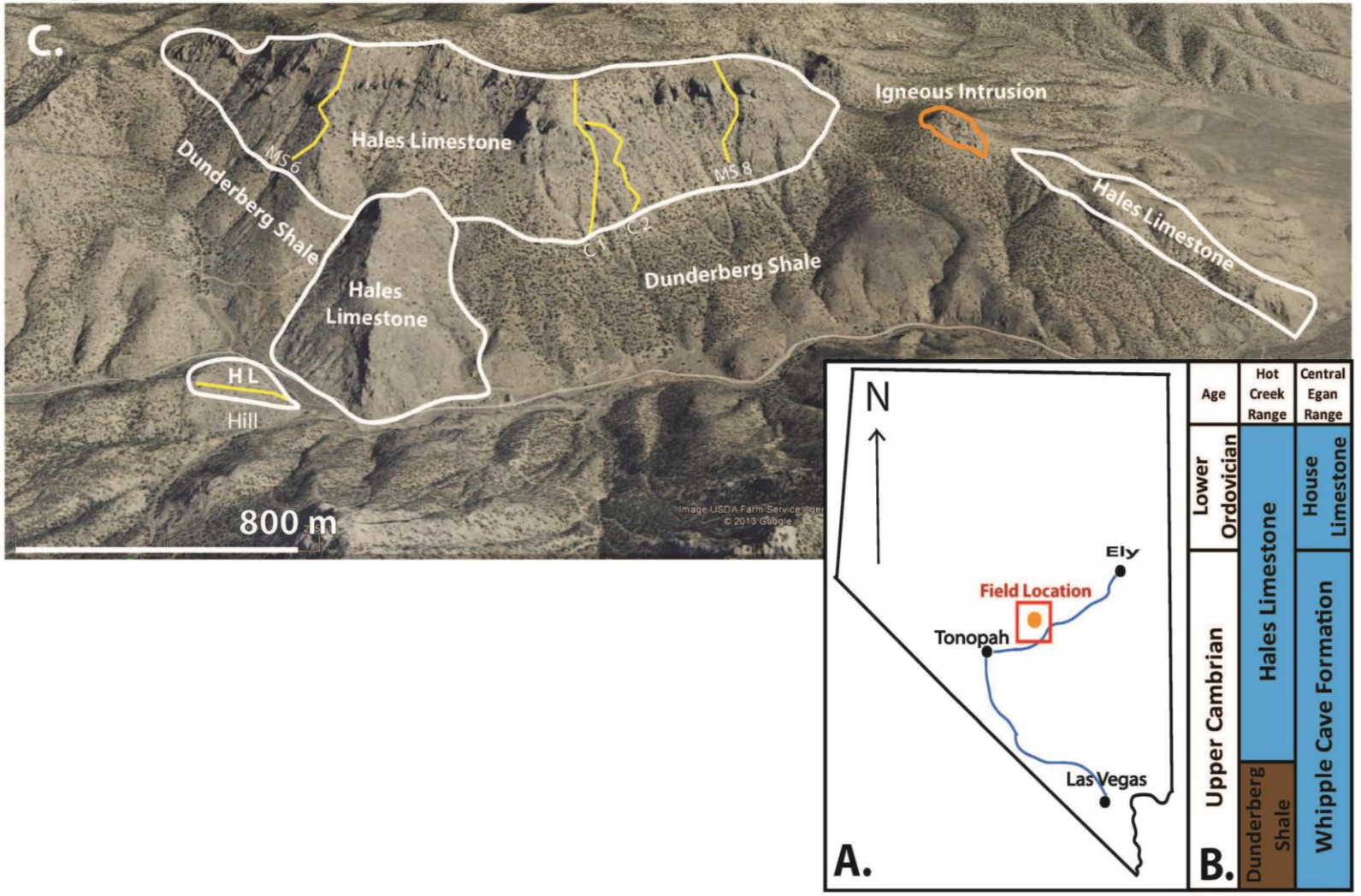

Figure 2

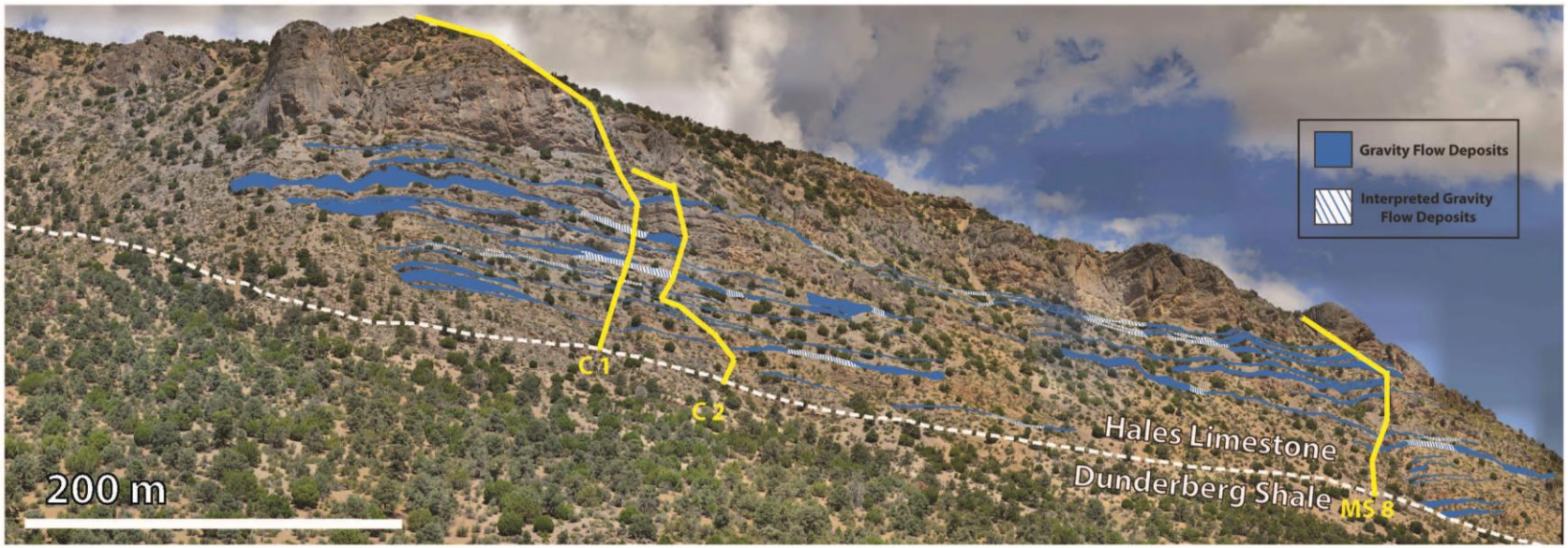
Gravity Flow Deposits
Interpreted Gravity Flow Deposits
C 1
C 2
Hales Limestone
Dunderberg Shale
MS 8
200 m

Figure 3

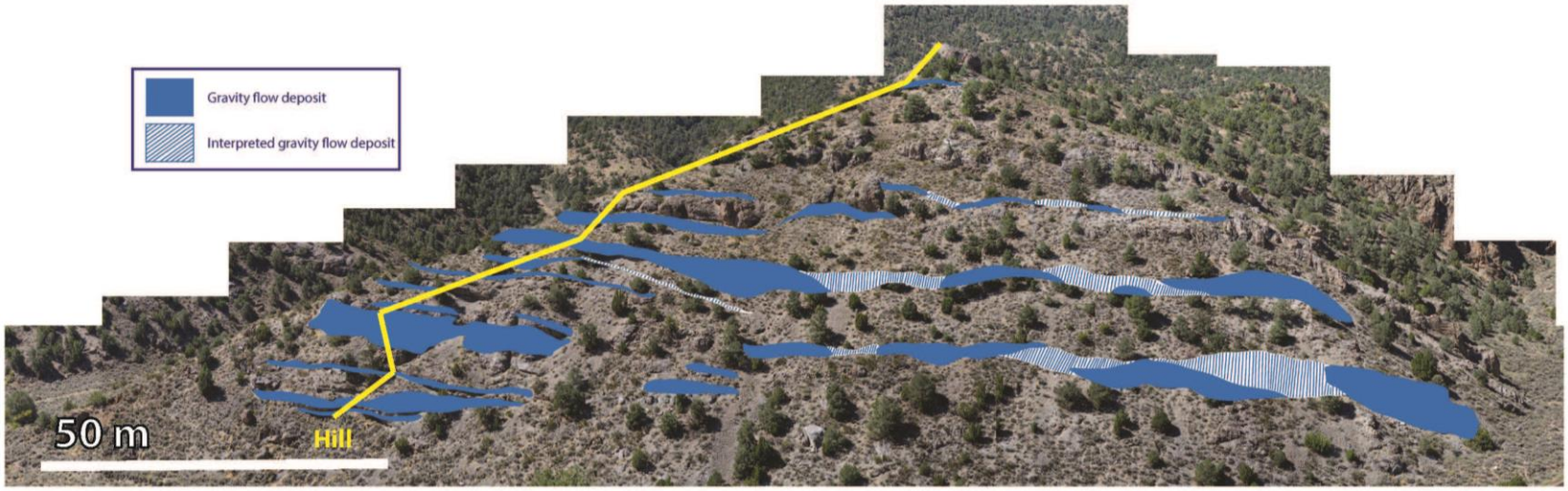
Gravity flow deposit
Interpreted gravity flow deposit
50 m
Hill

Figure 4

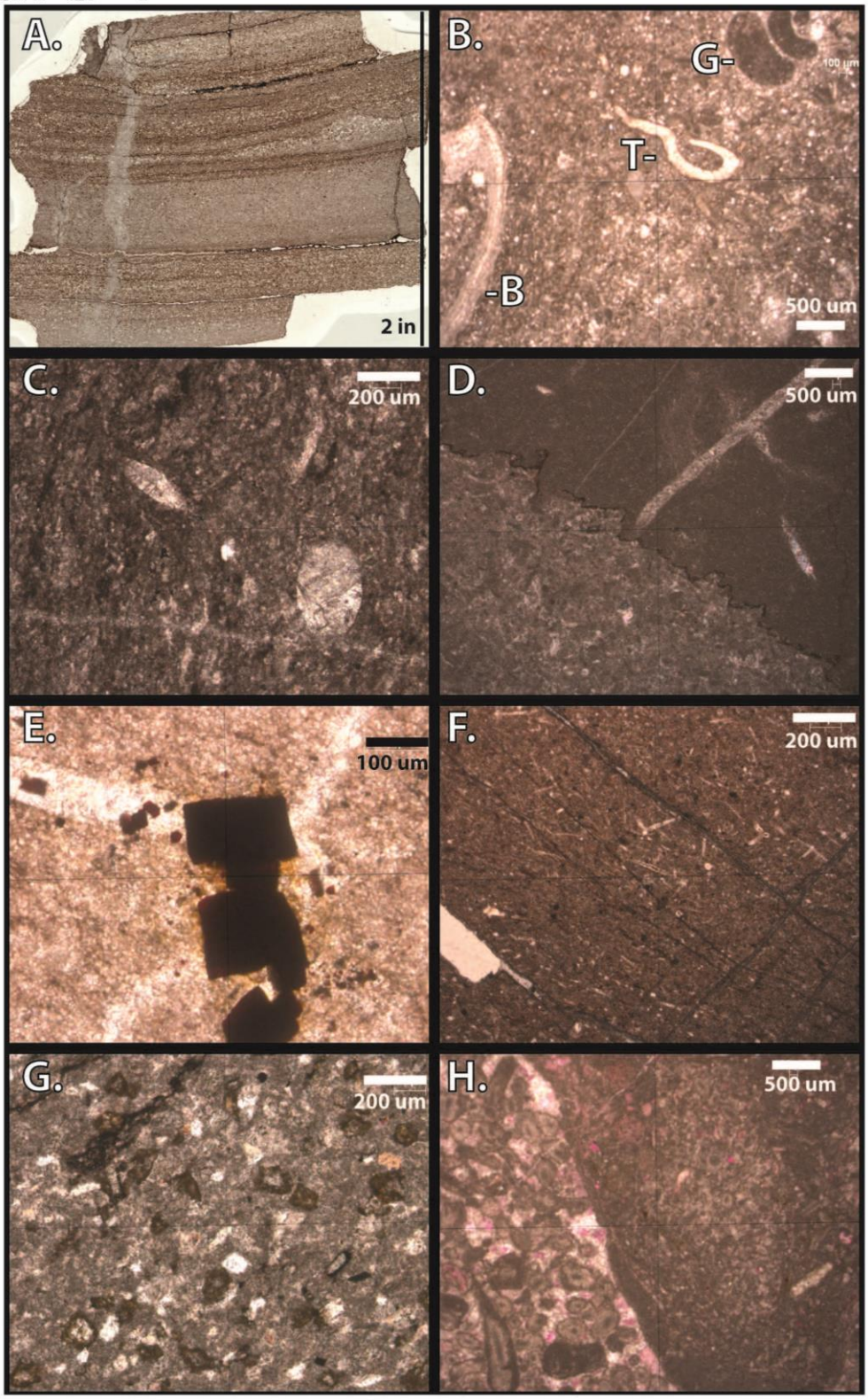
A.
2 in
B.
G-
T-
-B
100 um
500 um
C.
200 um
D.
500 um
E.
100 um
F.
200 um
G.
200 um
H.
500 um

Figure 5

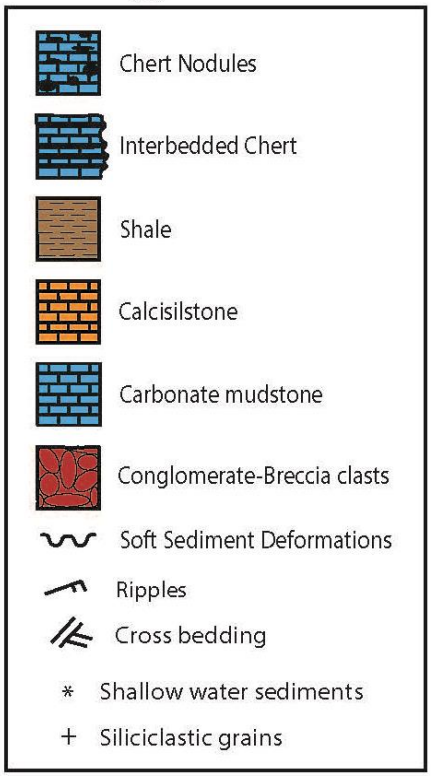
Chert Nodules
Interbedded Chert
Shale
Calcisilstone
Carbonate mudstone
Conglomerate-Breccia clasts
Soft Sediment Deformations
Ripples
Cross bedding
Shallow water sediments
Siliciclastic grains

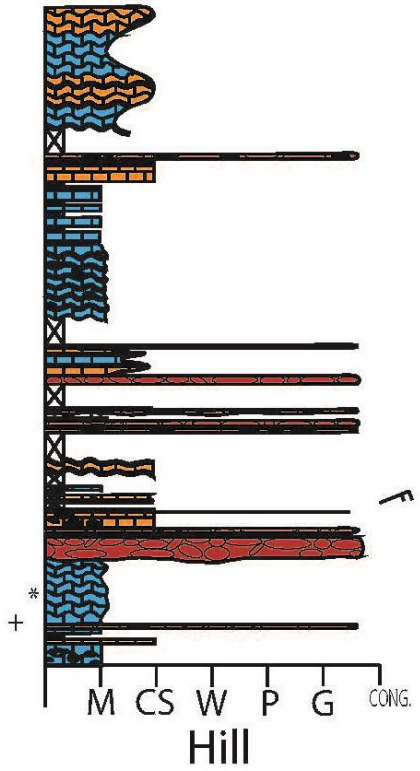
M CS W P G CONG.
Hill

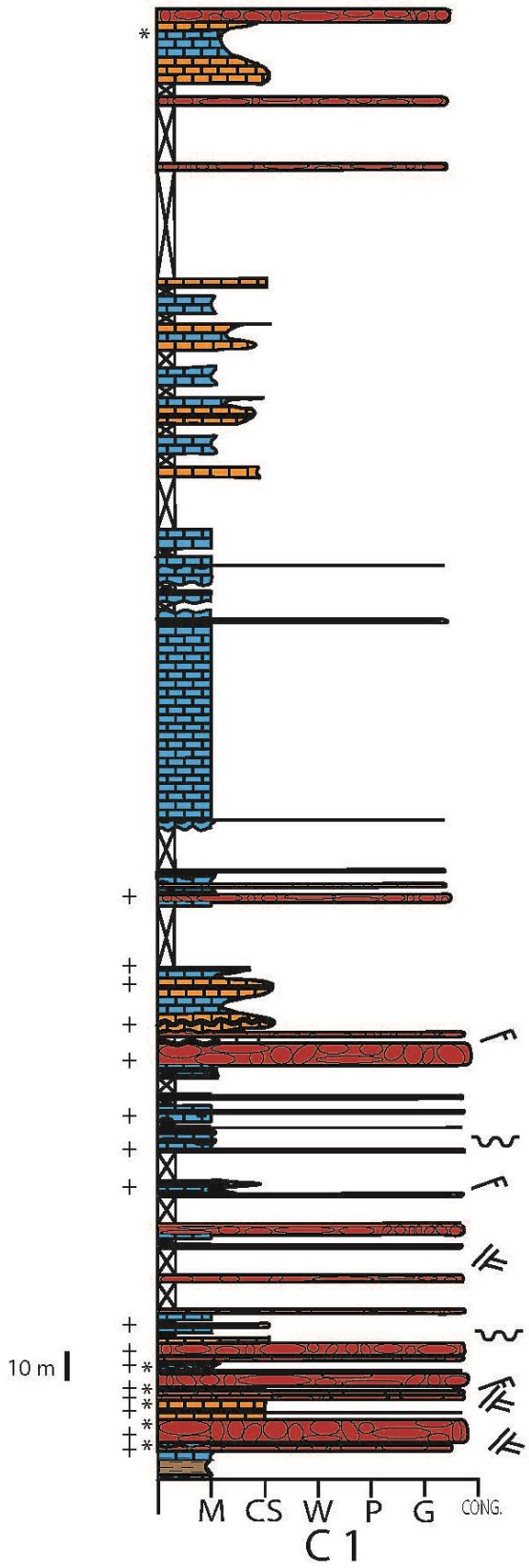
10 m
M CS W P G CONG.
C 1

Figure 6

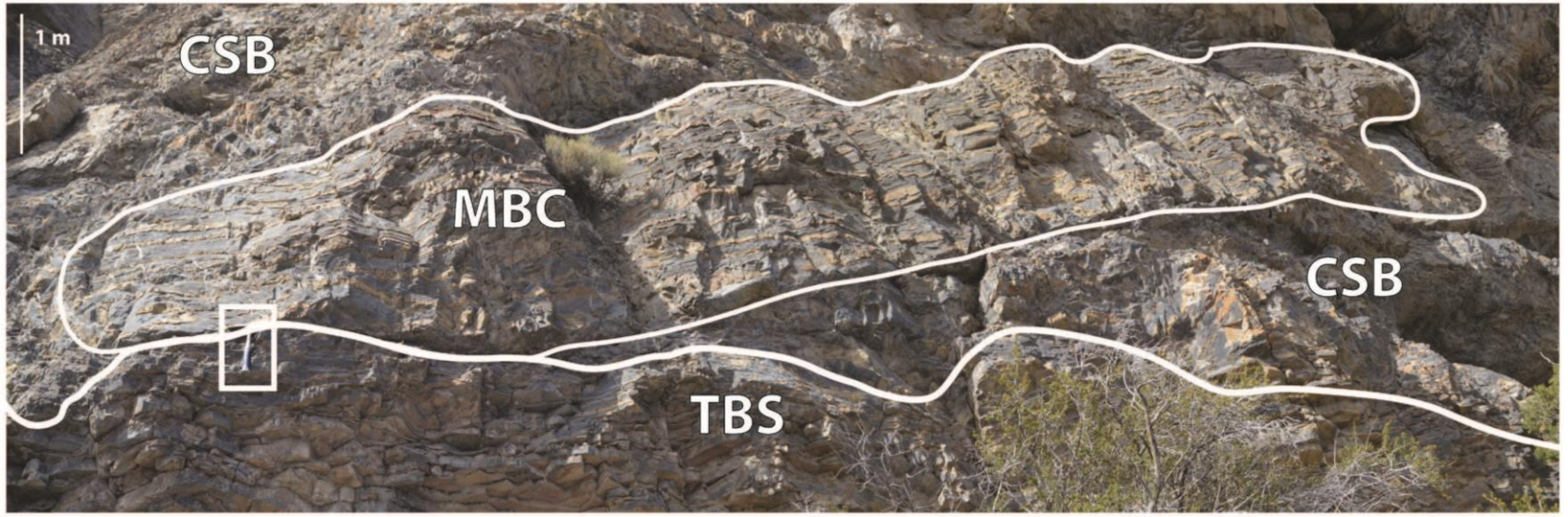

Figure 7

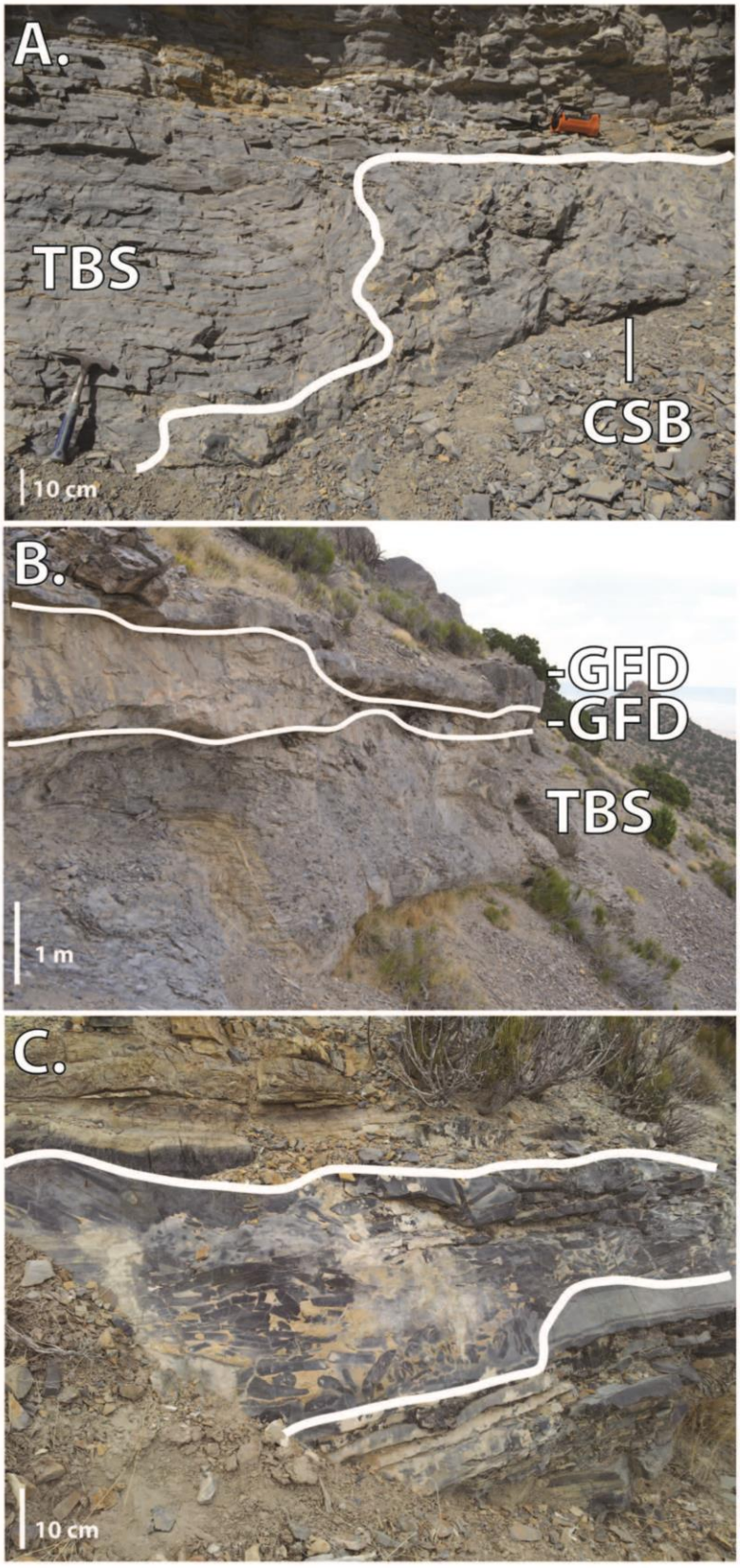

Figure 8

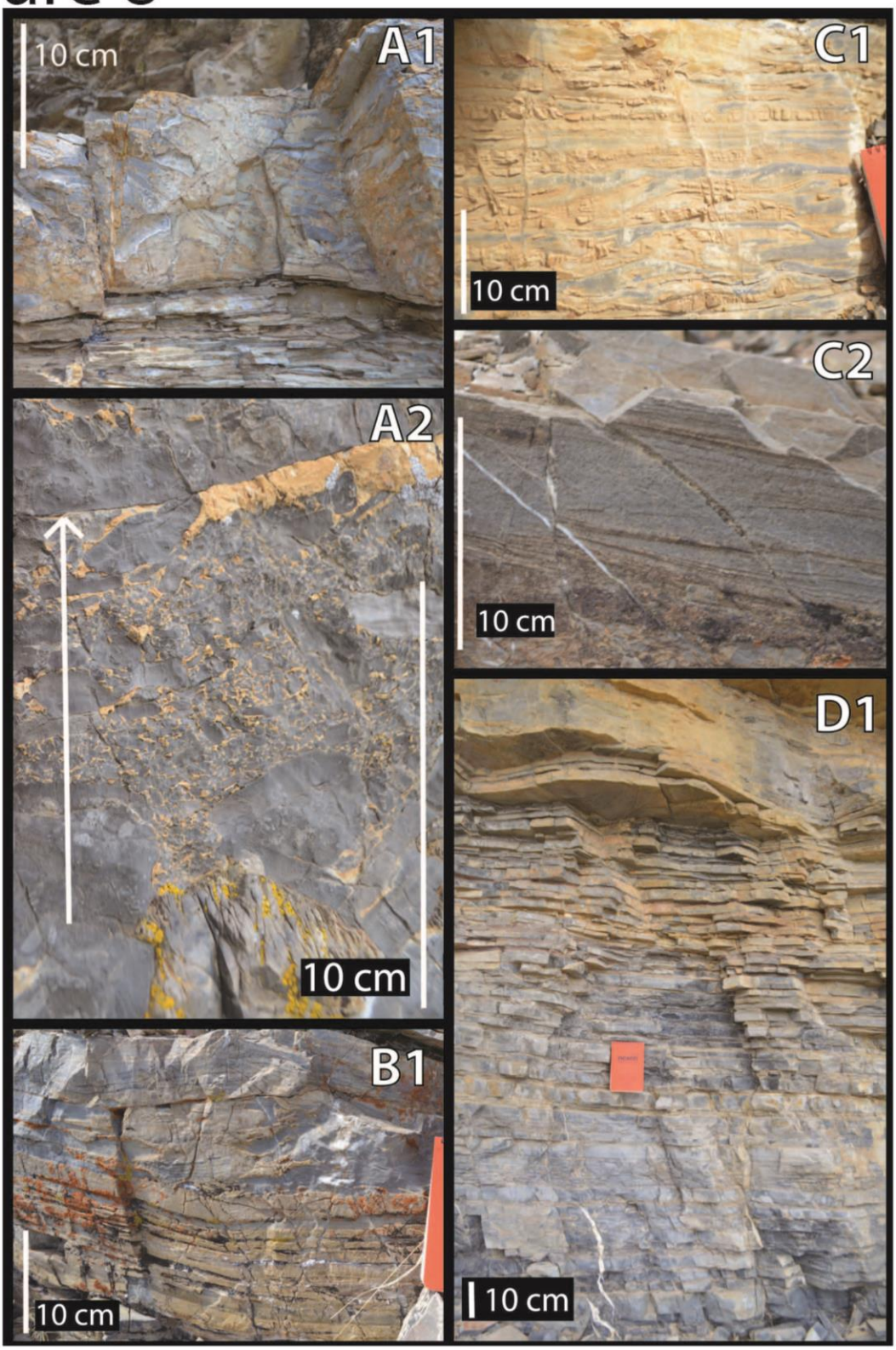

Figure 9

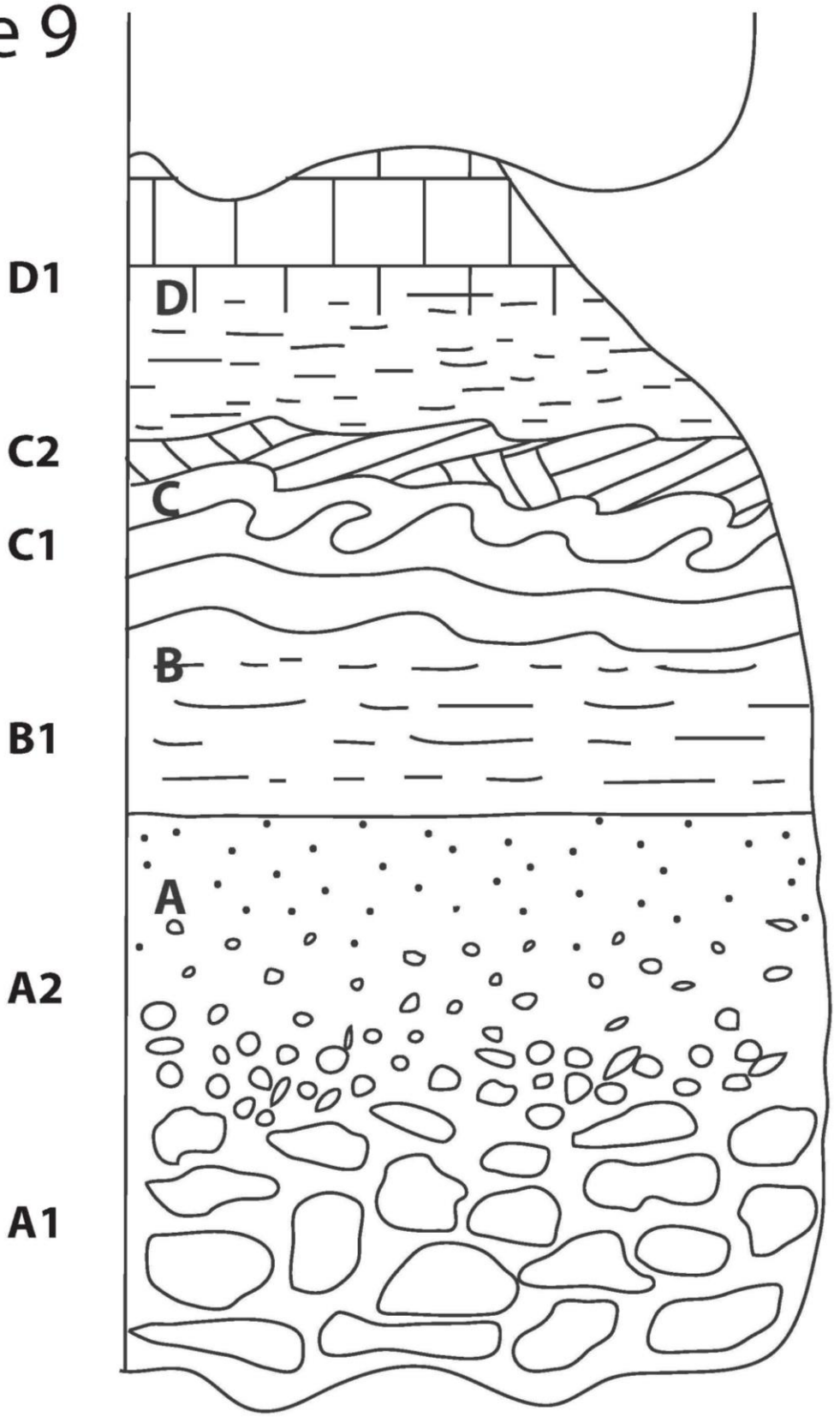

Figure 10

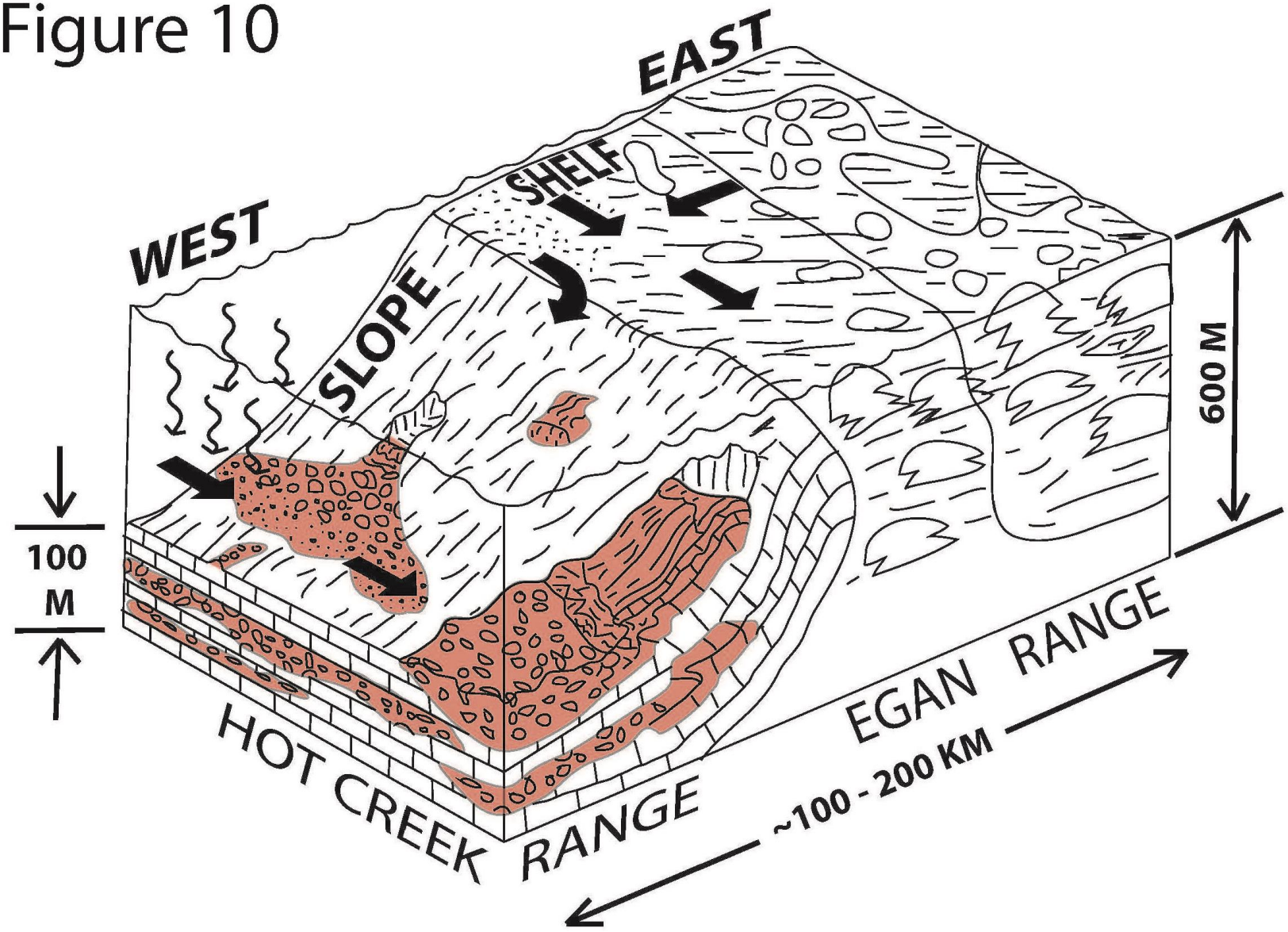
EAST
SHELF
WEST
SLOPE
600 M
100
M
HOT CREEK RANGE
EGAN RANGE
~100 - 200 KM

APPENDIX C

TABLES

TABLE 1 - Description of Hales Limestone Facies

Picture	Facies	Description	Interpretations
	(1a) Clast- and matrix-supported conglomerate -breccia beds	These beds range from 10 cm to 12 m thick. The majority of these beds range from 30 cm to 3 m thick. The conglomerate clasts are primarily composed of carbonate mudstone and calcisiltstone. The clasts are composed of semi-lithified sediment. These clasts range in size from pebbles, a few cm in length, to boulders, a few meters in length. The majority of these clasts range in size from pebbles to cobbles. Some clasts are composed of thin-bedded to laminated sediments composed of carbonate mudstone and calcisiltstone. The matrix of these beds is primarily composed of calcisiltstone. Carbonate mud and calcite also occur in the matricies of these beds. Brachiopod, trilobite, and other fossil fragments are present in some of these clast beds in both the clasts and the matrix. Silica is also present in some clast beds. Sedimentary structures in some of the beds show fining upwards sequences of clasts or normal grading and peloids. This facies composes between 14% and 30% of the Hales Limestone	The clast-supported conglomerate beds represent a high-energy environment that is the result of a gravity flow. These clasts are formed from semi-lithified sediment that were previously deposited on the slope and margin. These deposits typically indicate carbonate turbidites, and these beds show the first stage, A, of the carbonate turbidite sequence, a variation of the siliciclastic Bouma sequence.
	(1b) packstone - grainstone beds	These beds are primarily located on the east side of Tybo Canyon in Hot Creek Range. These deposits have a matrix composed of carbonate mudstone and calcite. The fossil packstone to grainstone beds contain brachiopods, trilobites, gastropods, crinoids, and peloids. These sediments also contain silica grains. These beds are highly fractured with calcite-filled veins and compose less than 1% of the Hales Limestone deposits.	These grain-supported beds represent a high-energy environment that resulted in grain flow deposits. These deposits originated in a shallow water environment.
	(2) Alternating thin, planar calcisilt and carbonate mud beds	These beds range from 1 m to 100 m thick. The beds are planar, alternating layers composed of carbonate mud and calcisilt. There are also silica grains, chert, calcispheres, pyrite, and ankerite sediments in these layers. Some of these sediments have a graded abundance, while others are scattered throughout the sediment layers. Brachiopod, gastropod, crinoid, trilobite, spicule fossils and fragments occur in some of these layers. Horizontal burrows also occur in some of the sediment layers. Soft sediment deformation, load structures, reverse grading, and styolites also occur within these beds. This facies comprises between 20% and 40% of the Hales Limestone.	The alternating calcisiltstone and mudstone layers represent the second stage, B, of the carbonate turbidite sequence, a variation of the siliciclastic Bouma sequence. This facies was deposited in lower energy environment than that clast-supported beds, but it was still deposited in a high-energy environment.

	(3) Wavy and cross-bedded mudstone and calcisiltstone	These beds range from 50 cm to 1 m thick. They are composed of calcisiltstone and carbonate mud sediments intermixed. These thin-bedded sediments contain sedimentary structures such as cross bedding, climbing ripples, wavy laminations, and convoluted bedding. These sedimentary features are primarily composed of calcisiltstone sediments. These beds often occur above the conglomerate beds. This facies comprises less than 5% of the Hales Limestone.	The wavy and cross-bedded deposits represent the third stage, C, of the carbonate turbidite sequence, a variation of the siliciclastic Bouma sequence. The variation of carbonate mudstone and calcisiltstone shows the movement in the environment created by the high-energy.
	(4) Thin planar mudstone	These beds range from 2 cm to 10 cm thick. These are planar beds that range from thin to thick bedded layers of carbonate mud. There are also interbedded chert nodules and layers of chert within the carbonate mud. Crinoids, calcispheres, and spicules occur within these sediments. Sedimentary structures in these sediments include folds, slumps, soft sediment deformation, and stylolites. This facies comprises between 35% and 60% of the Hales Limestone.	These beds are deposited in a calm, low-energy environment. The thin to thick planar mudstone represents the fourth stage, D, of the carbonate turbidite sequence, a variation of the siliciclastic Bouma sequence. These beds also indicate the background sedimentation of pelagic carbonate mudstone on the slope to toe-of-slope environment.
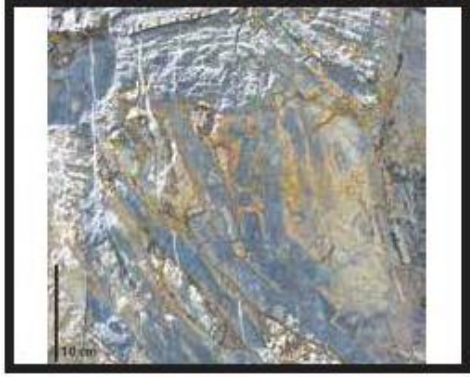	(5) Deformed beds	These beds range from 1 m to 10 m thick. These beds of carbonate mud and calcisiltstone contain folded and slumped beds amongst thin-bedded sediments. There are also chert nodules and layers present in some of these beds. Some of the thin beds are broken indicating syndepositional movement of the sediment layers. The movement can show significant deformation to very little movement of the thin-bedded layers. This facies comprises less than 1% of the Hales Limestone.	The deformed beds represent the movement that occurs at the beginning of a gravity flow. The folding and slumping of the beds indicates the dewatering process of the sediments was enough to cause slope failure, but the movement was insufficient to cause significant movement of the semi-lithified sediments, such as that seen in the clast-supported conglomerate beds.

APPENDIX D

Figure A-1: Soft sediment deformation of carbonate mudstone into calcisiltstone.

Figure A-2: Multiple sequences of fining-upwards carbonate mudstone clasts in a calcisiltstone matrix.

Figure A-3: Imbricated carbonate mudstone clasts in a calcisiltstone matrix, overlain by interbedded carbonate mudstone and calcisiltstone.

Figure A-4: Carbonate mudstone clasts deposited within a previously-deposited carbonate mudstone clast.

Figure A-5:Burrows (trace fossils) in a carbonate mudstone layer at the top of the Hales Limestone outcrop in Tybo Canyon.

Figure A-6: Carbonate mudstone clasts in a calcisiltstone matrix, overlain by calcisiltstone climbing ripples, which are subsequently overlain by interbedded carbonate mudstone and calcisiltstone and another bed of carbonate mudstone clasts in a calcisiltstone matrix.

Figure A-7: Channel-like deposits composed of carbonate mudstone clasts and calcisiltstone matrix, overlain by another sequence of larger carbonate mudstone clasts in a calcisiltstone matrix.

Figure A-8: Chert nodule in carbonate mudstone.

Figure A-9: Fining upwards clasts of carbonate mudstone in a calcisiltstone matrix.

Figure A-10: Coarsening upwards sediments from carbonate mudstone to calcisiltstone, overlain by carbonate mudstone clasts in a calcisiltstone matrix.

Figure A-11: Interbedded carbonate mudstone and chert.

Figure A-12: Monoclinal fold, soft sediment deformation of interbedded layers of carbonate mudstone and calcisiltstone.

Figure A-13: Large clast of thin-bedded carbonate mudstone within a larger gravity flow deposit composed of carbonate mudstone clasts in a primarily carbonate mudstone matrix.

Figure A-14: Carbonate mudstone clasts in a calcisiltstone matrix, overlain by a layer of calcisiltstone.

Figure A-15: Graded contact of the underlying Dunderberg Shale formation with the overlying carbonate mudstone of the Hales Limestone formation.

Figure A-16: Climbing ripples in layers of interbedded carbonate mudstone and calcisiltstone.

Figure A-17: Several layers of beds with carbonate mudstone clasts and calcisiltstone matricies, divided by thin-bedded layers of carbonate mudstone.

Figure A-18: Scanned thin section of a peloidal brachiopod grainstone.

Figure A-19: Scanned thin section of alternating light and dark bands of carbonate mudstone. It shows small-scale soft sediment deformation.

Figure A-20: Scanned thin section of carbonate mudstone. Dark lines are insoluble residue, which are often points of fracture. The white sediments are silica grains.

Figure A-21: Scanned thin section of a peloidal grainstone.

APPENDIX E

Figure A-1

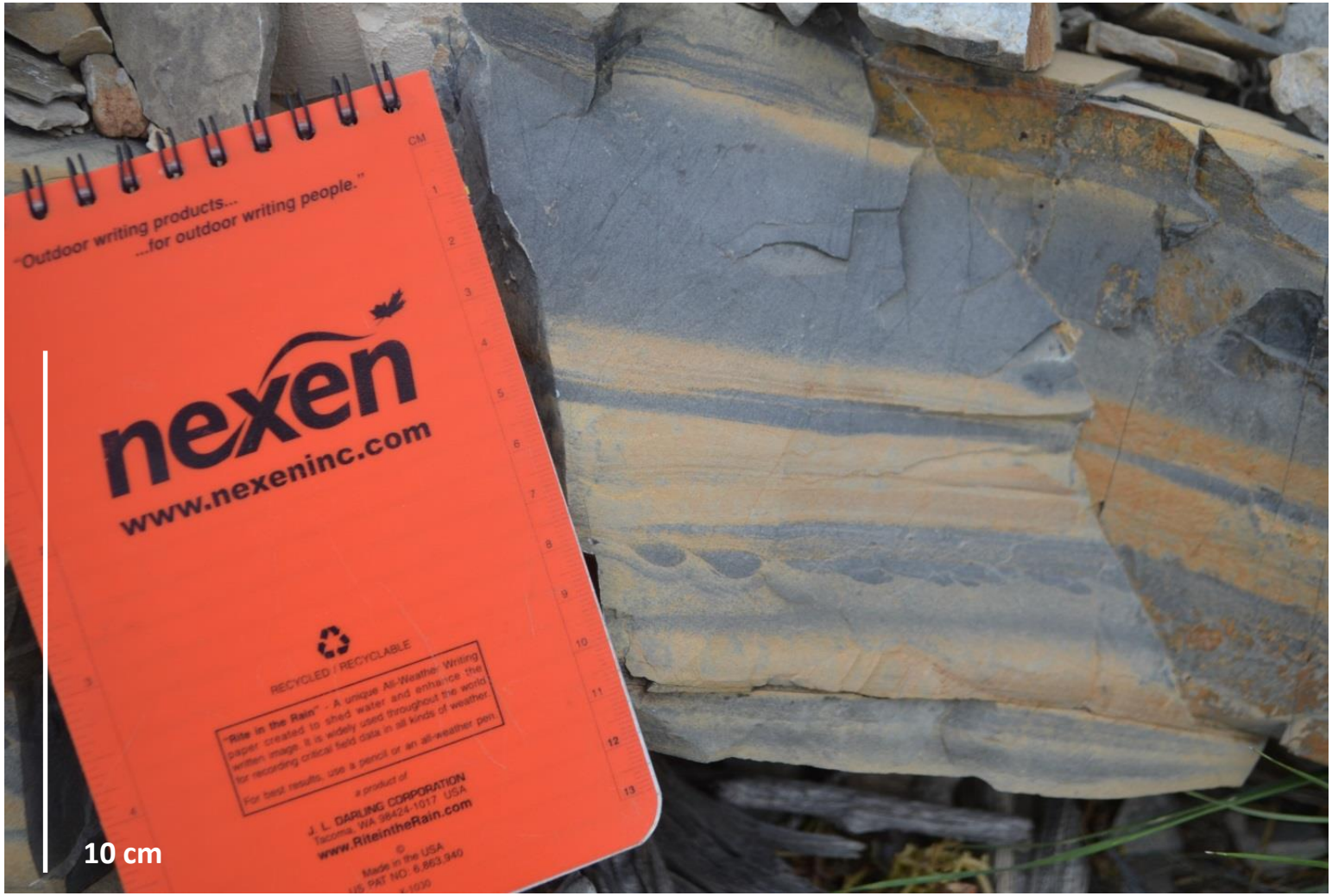

Figure A-2

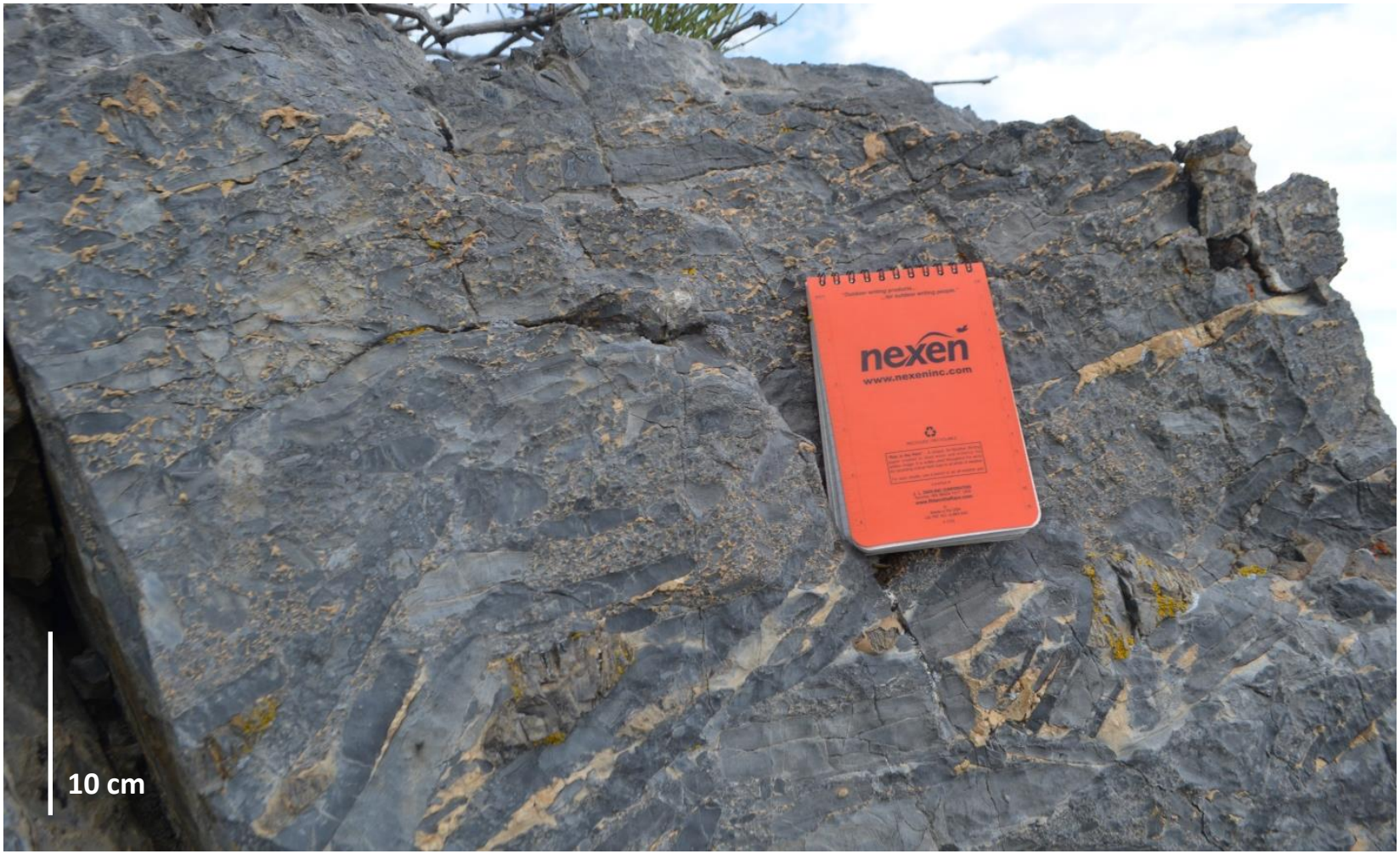

Figure A-3

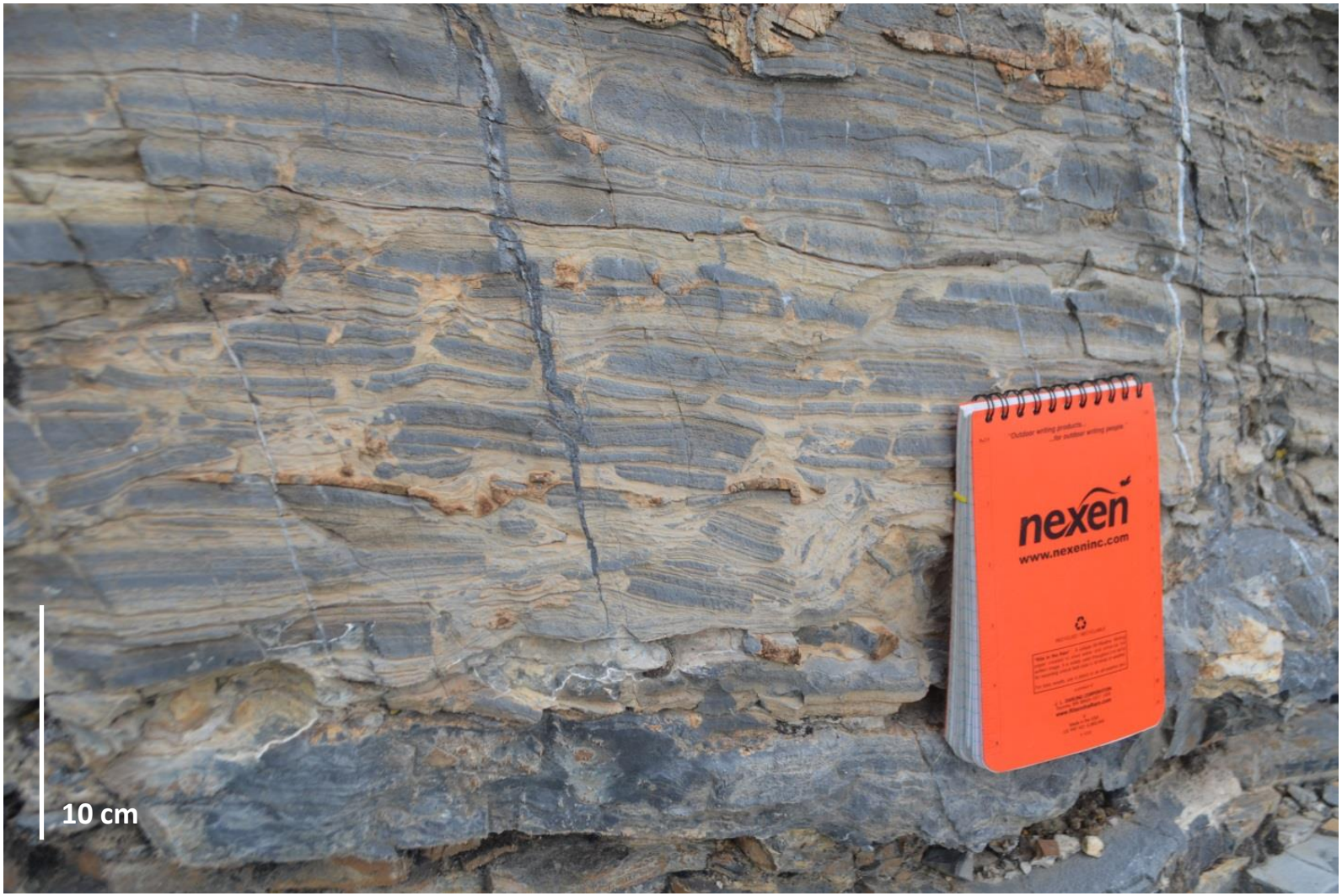

Figure A-4

Figure A-5

Figure A-6

Figure A-7

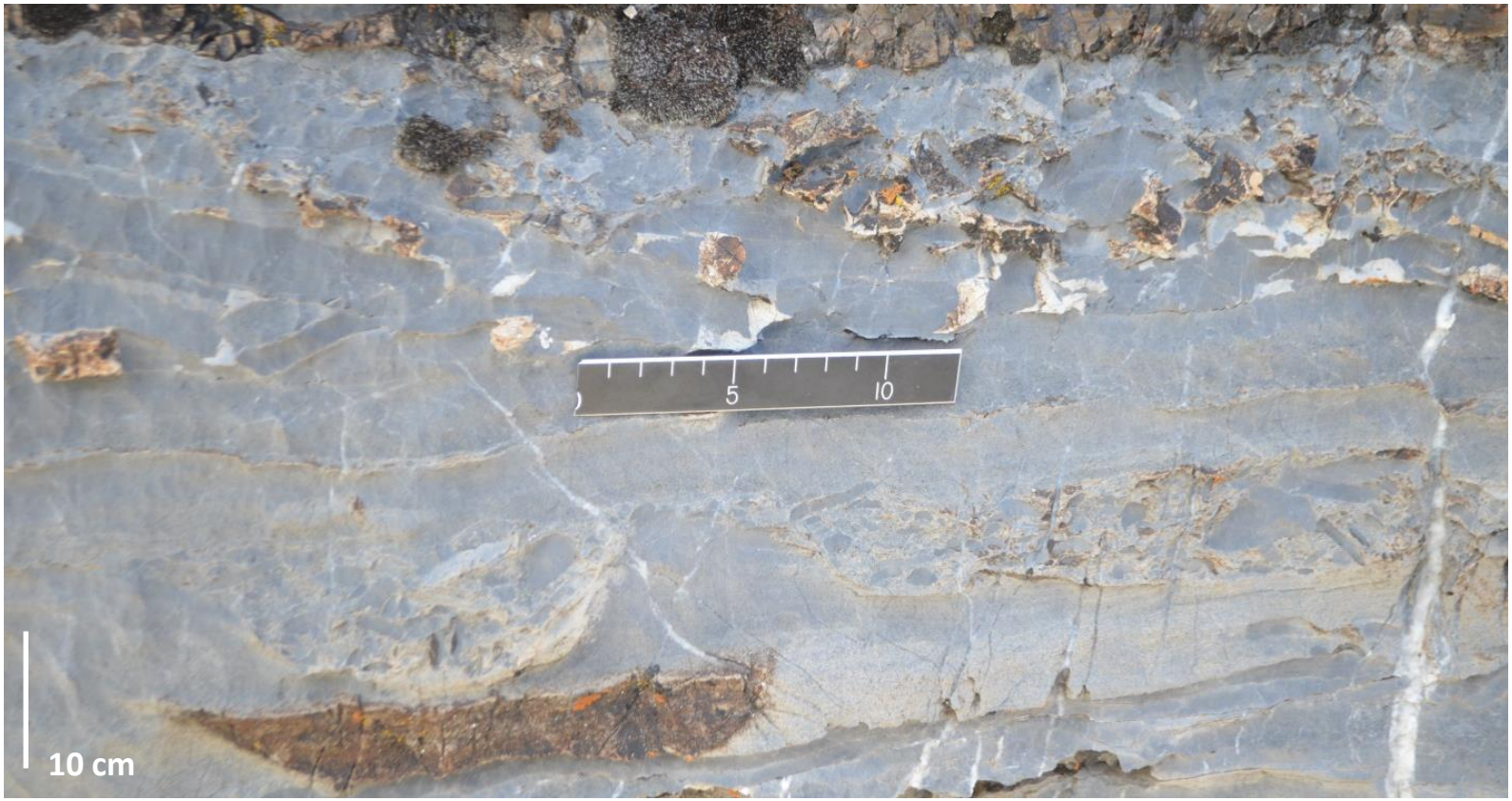

Figure A-8

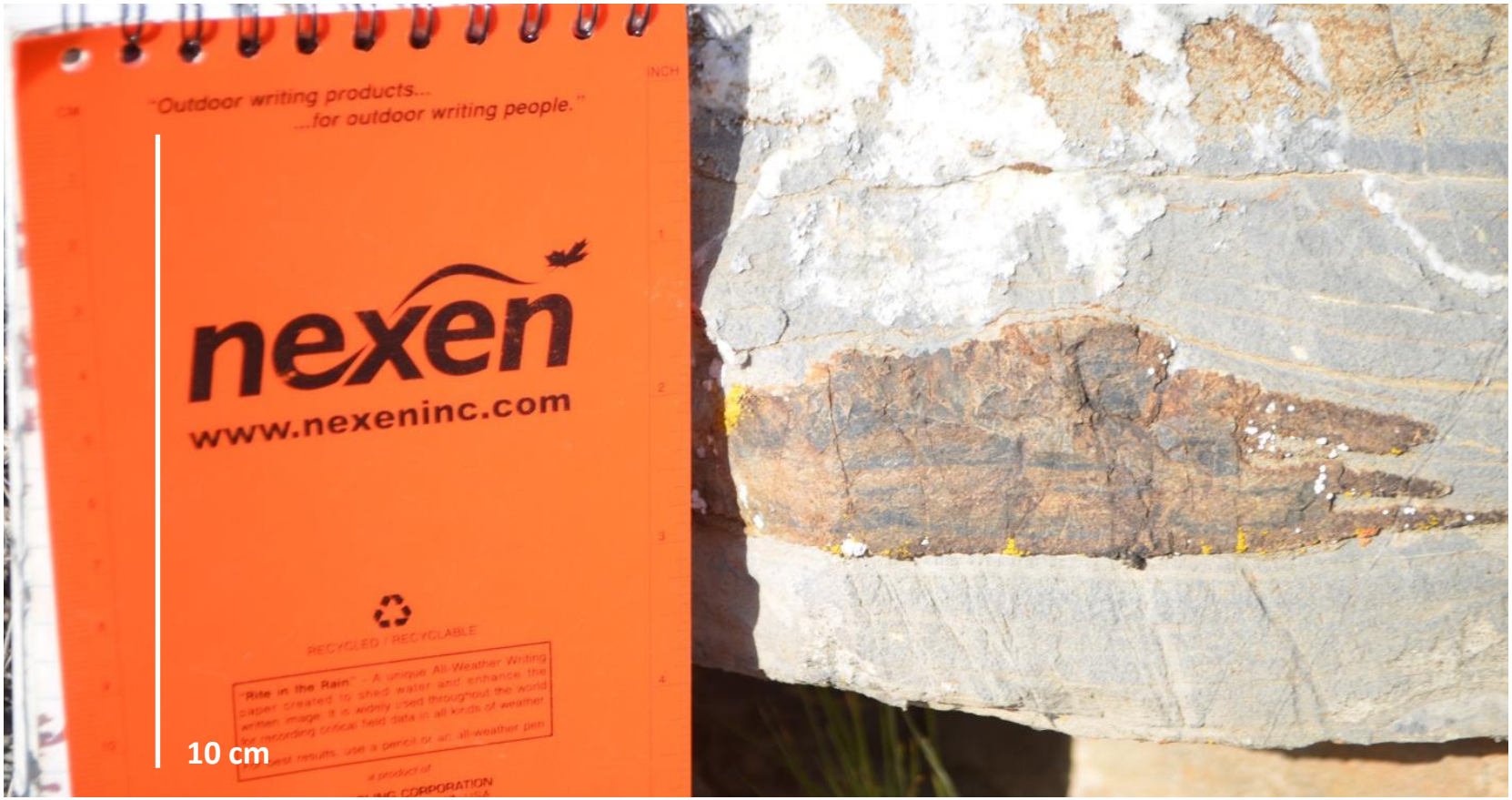
"Outdoor writing products...
...for outdoor writing people."
nexen
www.nexeninc.com
RECYCLED / RECYCLABLE
10 cm

Figure A-9

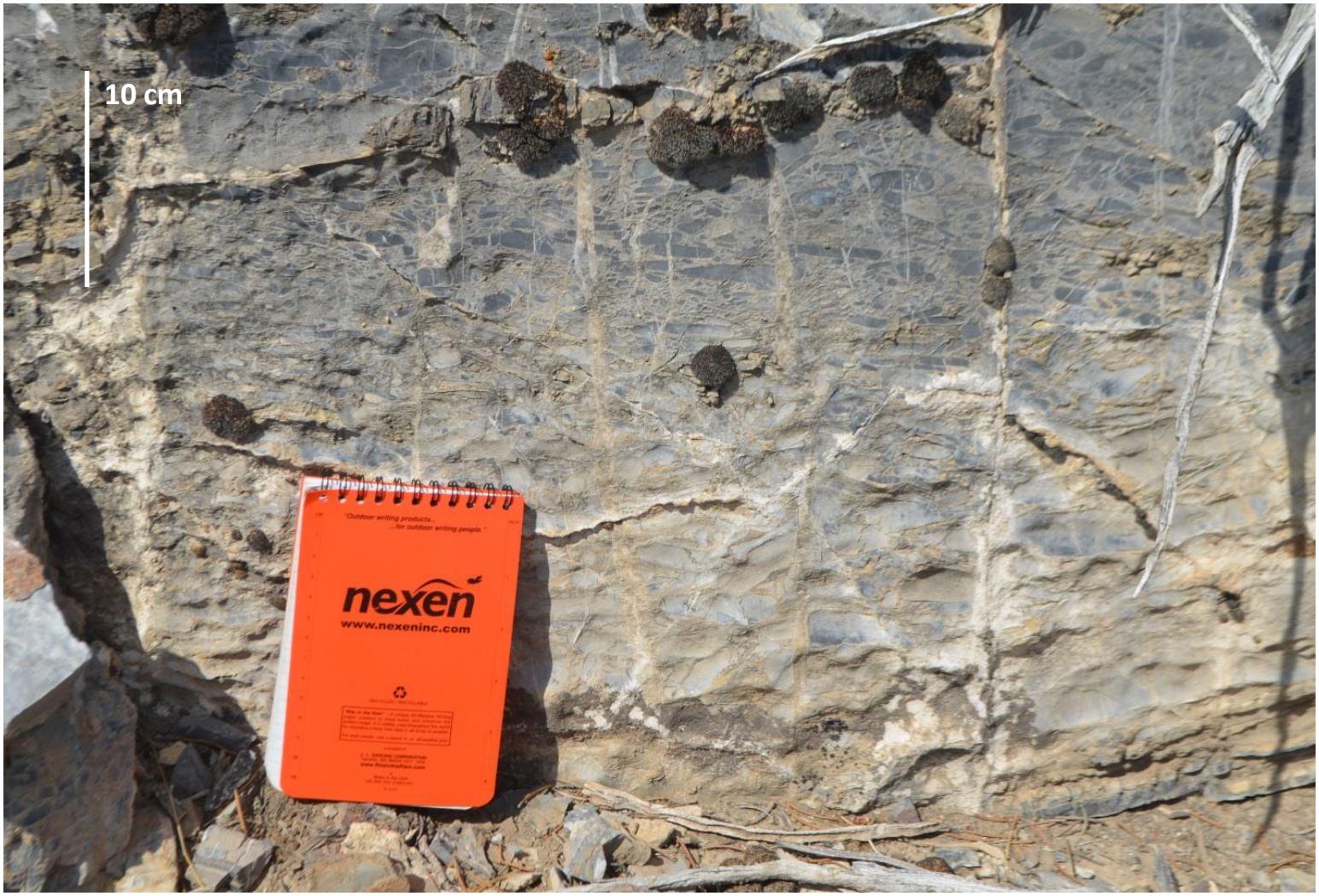

Figure A-10

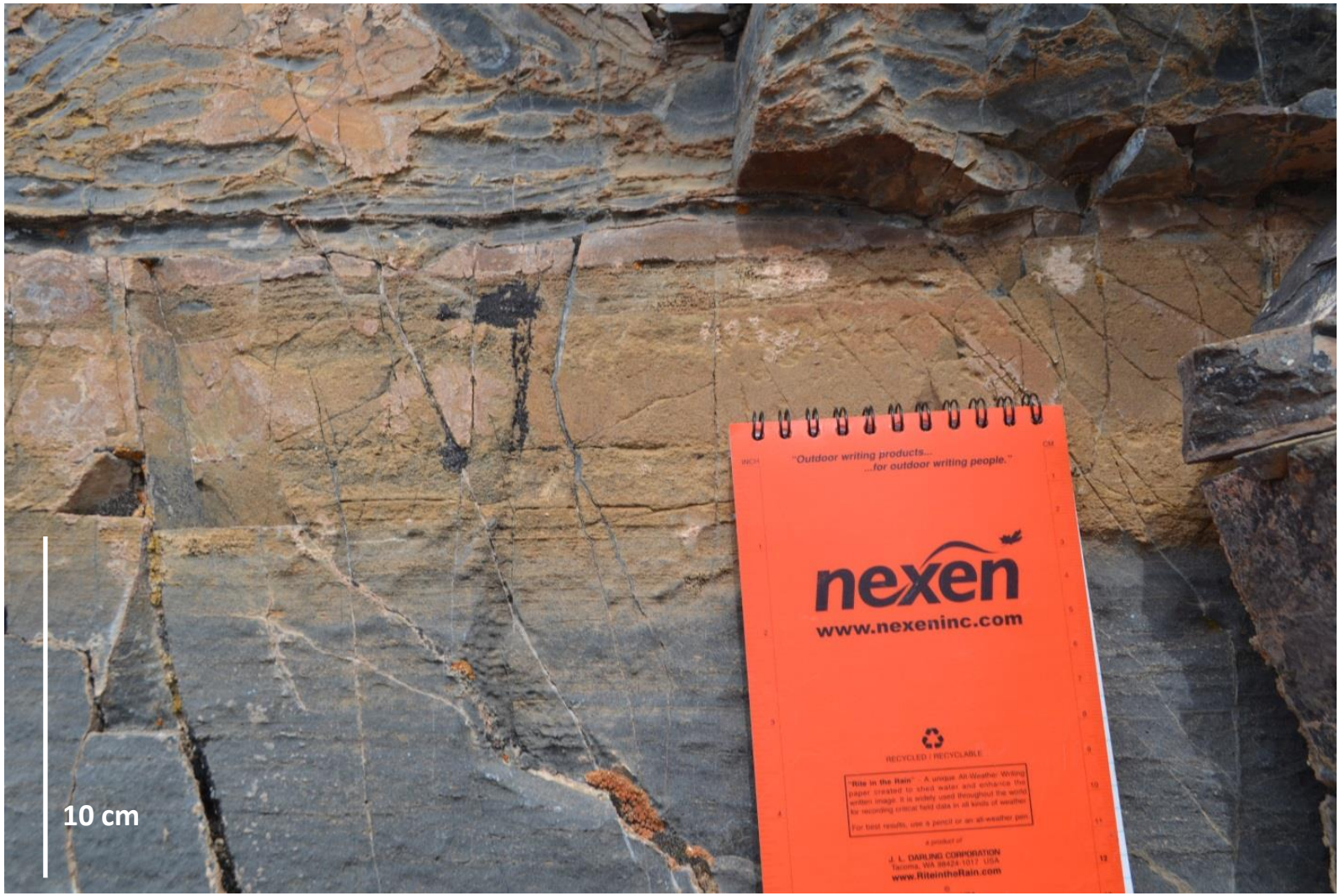
10 cm
"Outdoor writing products...
...for outdoor writing people."
nexen
www.nexeninc.com
RECYCLED / RECYCLABLE
"Rite in the Rain" - A unique All-Weather Writing paper created to shed water and enhance the written image. It is widely used throughout the world for recording critical field data in all kinds of weather.
For best results, use a pencil or an all-weather pen.
J. L. DARLING CORPORATION
Tacoma, WA 98424-1017 USA
www.RiteintheRain.com

Figure A-11

Figure A-12

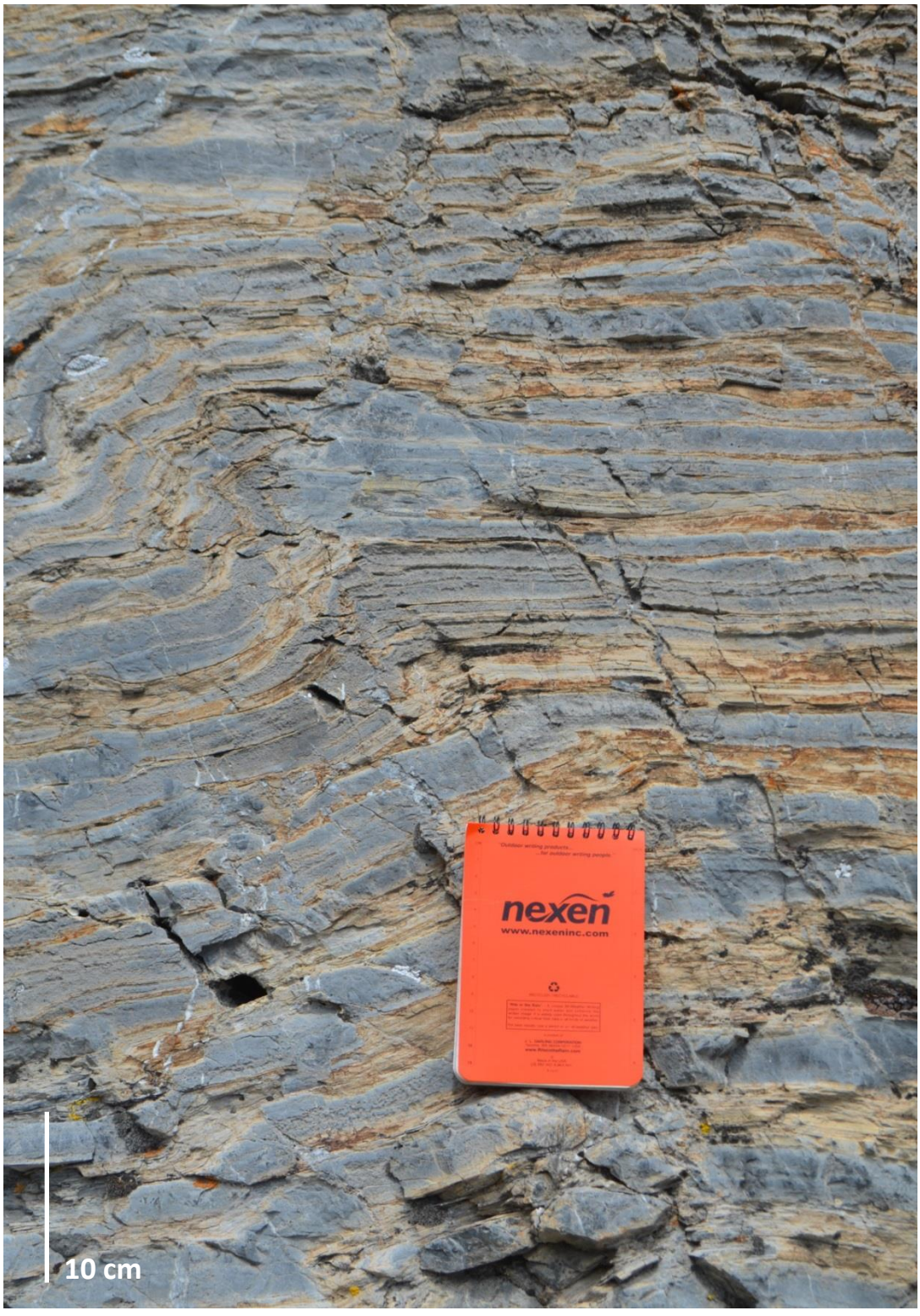

Figure A-13

Figure A-14

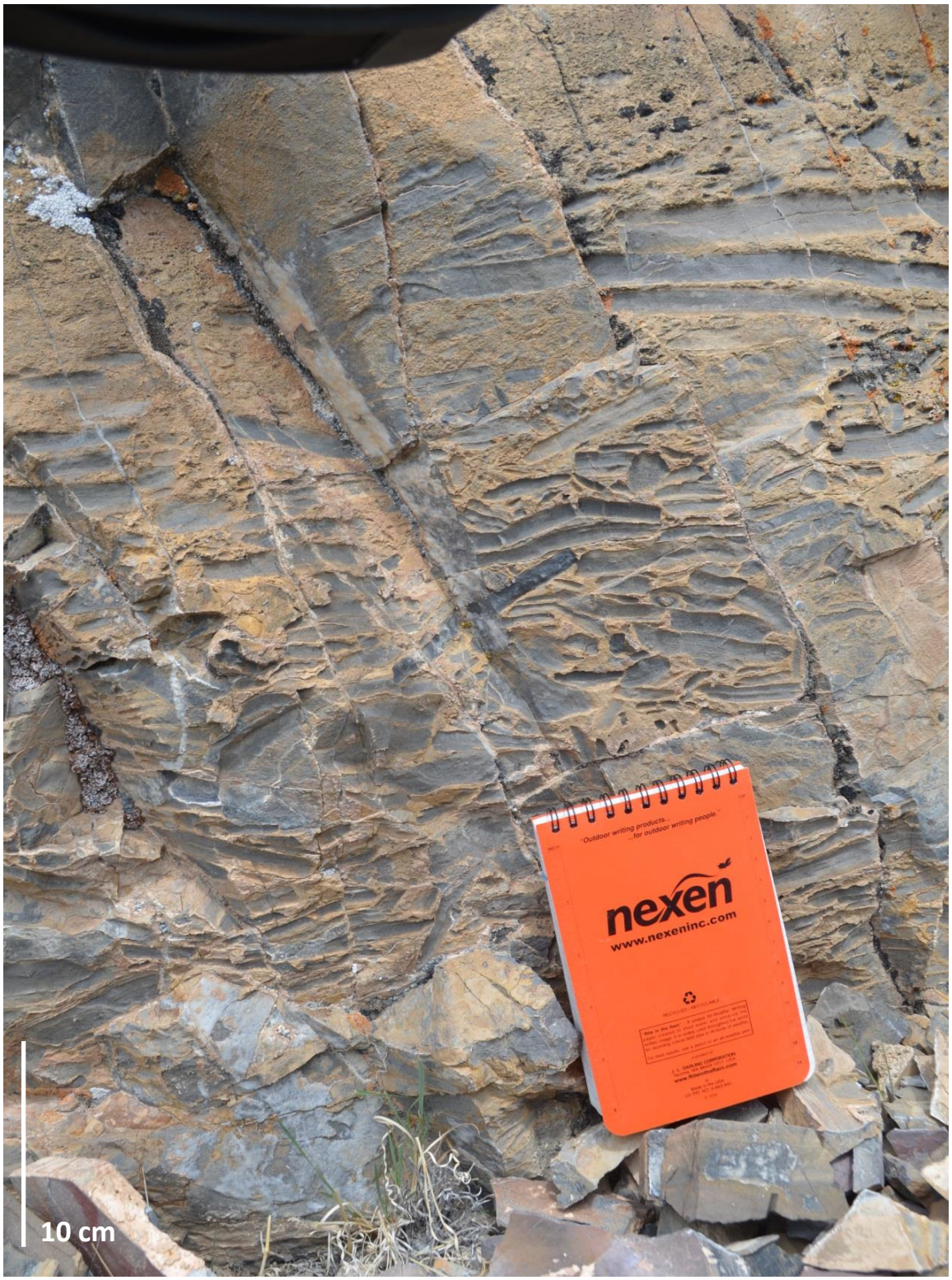
Outdoor writing products...
...for outdoor writing people
nexen
www.nexeninc.com
10 cm

Figure A-15

Figure A-16

Figure A-17

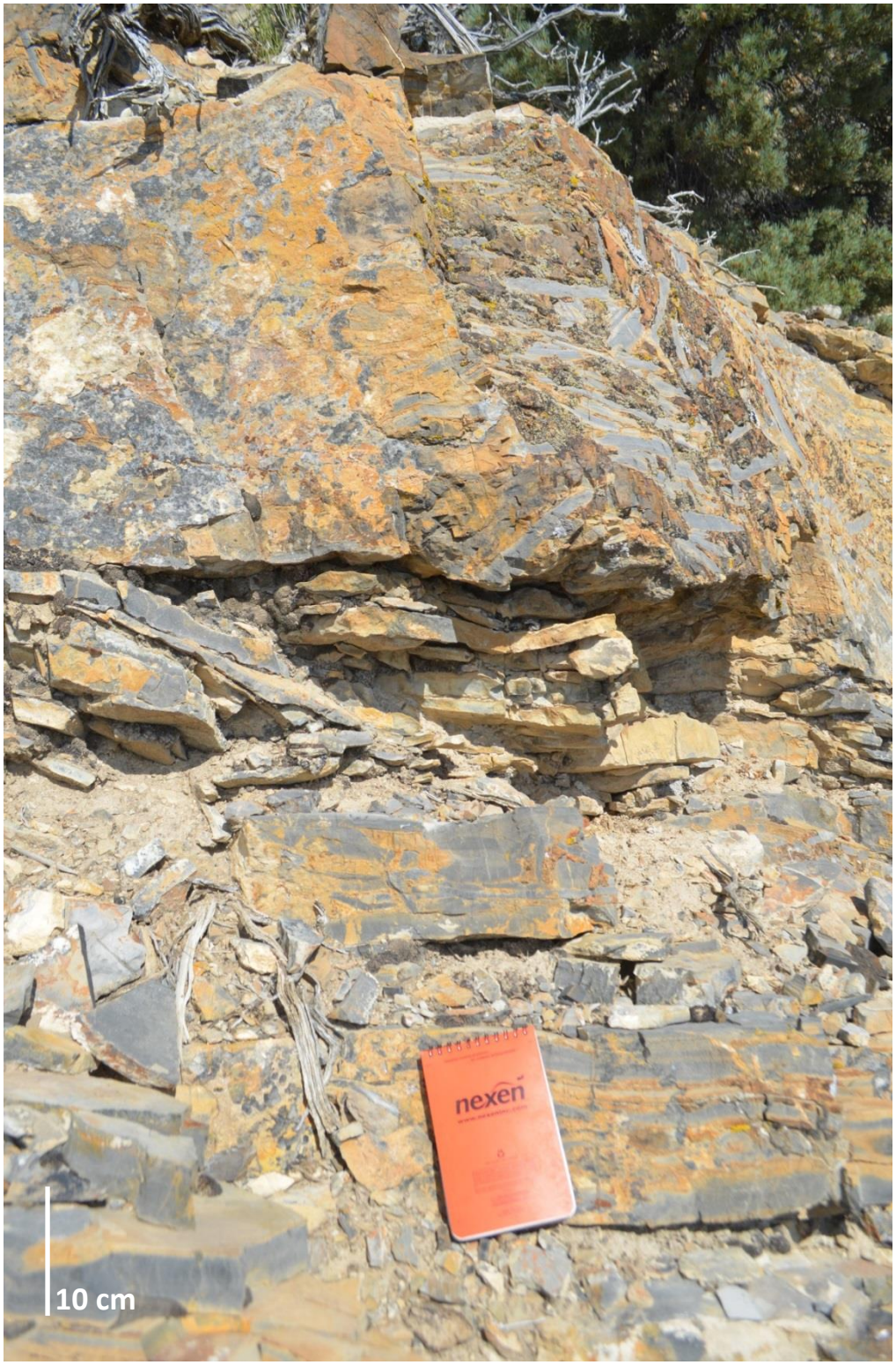

Figure A-18

Figure A-19

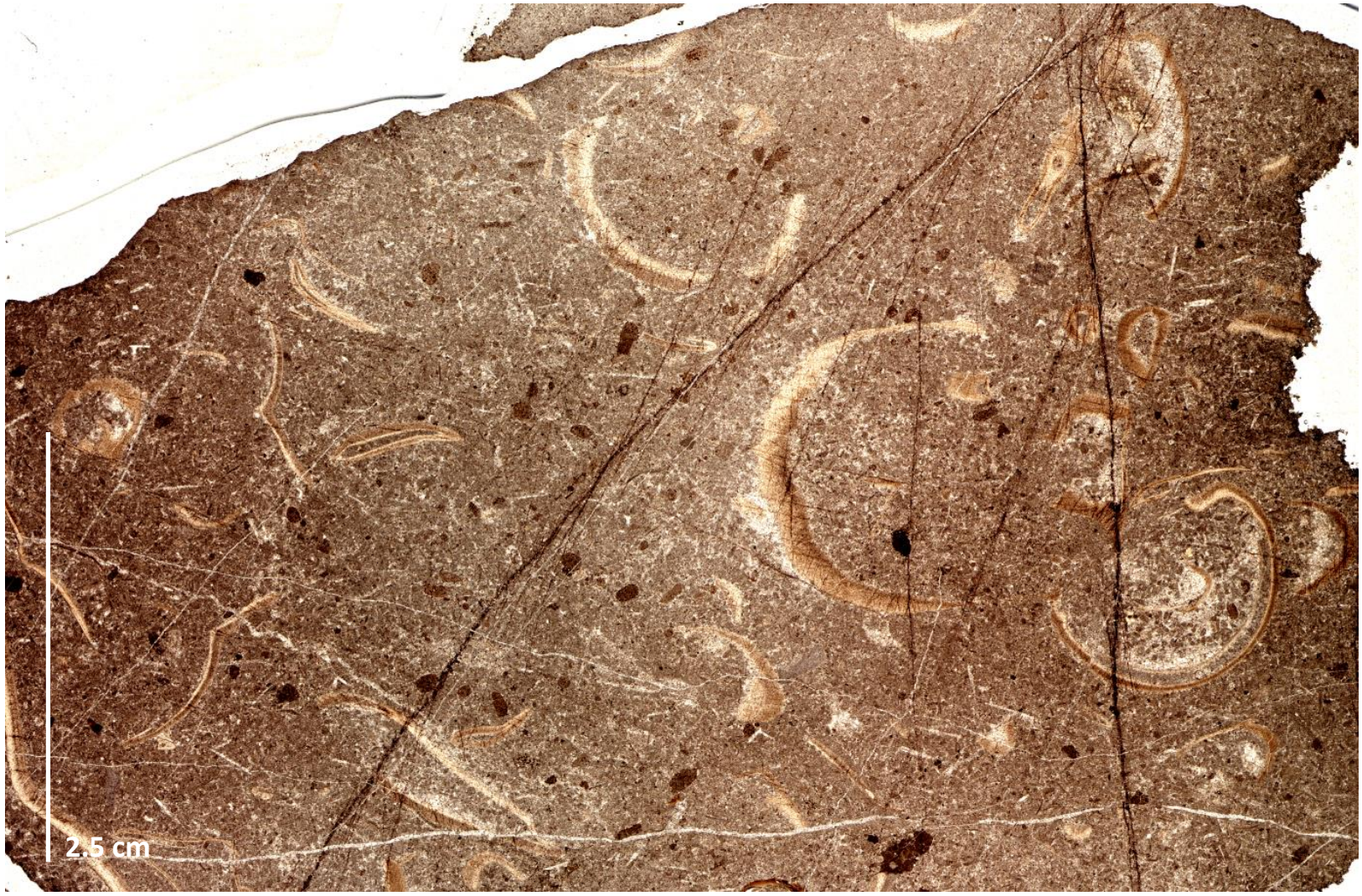

Figure A-20

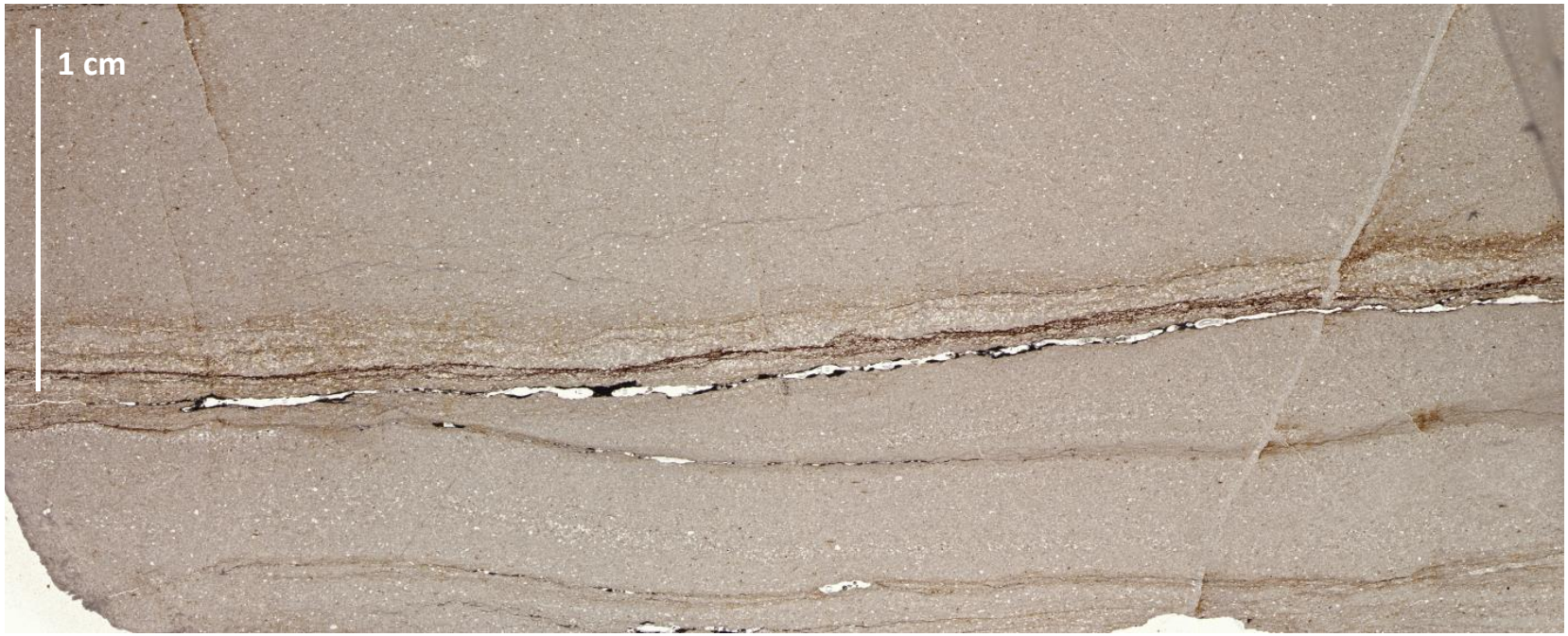

Figure A-21

TABLE 2- Measured Section GPS Coordinates		
Measured Section	Top	Bottom
C 1	11S 0552581 UTH 4247507	11S 0552544 UTH 4247934
C 2	11S 0552752 UTH 4247565	11S 0552461 UTH 4247889
Hill 1	11S 0551935 UTH 4246757	11S 0551667 UTH 4246748
MS 6	11S 0551656 UTH 4247674	11S 0551812 UTH 4248050
MS 8	11S 0553152 UTH 4247817	11S 0553097 UTH 4248074